# Phase diagrams and critical behavior in Ising square lattices with nearest- and next-nearest-neighbor interactions

K. Binder
*Institut für Festkorperforschung, der Kernforschungsanlage, Jülich, 5170 Jülich, Postfach 1913, West Germany*

D. P. Landau
*Department of Physics and Astronomy, University of Georgia, Athens, Georgia 30602*

(Received 7 May 1979)

The phase diagrams of Ising antiferromagnets in a magnetic field $H$ are investigated for various values of the ratio $R$ between nearest- and next-nearest-neighbor interaction. While mean-field approximations and the existing real-space renormalization-group treatments yield phase diagrams which are sometimes even qualitatively incorrect, accurate results are obtained from Monte Carlo calculations. For $R<0$ only an antiferromagnetically ordered phase exists. Its transition to the disordered phase is first order for temperatures below the tricritical point $(T_t, H_t)$. For $R \to 0$ also $T_t \to 0$. For $R=0$ we find very good agreement with the results of Müller-Hartmann and Zittartz. For $R>0$ and $H_1 < H < H_2$ a new phase with anomalous high ground-state degeneracy is found (two sublattices have only one-dimensional order). These sublattices undergo order-disorder transitions at $T=0$, such that for $T>0$ one is left with a "superantiferromagnetic" phase. At low temperatures in this phase a pronounced tendency is observed to form a simpler $(2\times 2)$ superstructure but with many antiphase domain boundaries. For $R \to \frac{1}{2}$ and $H < H_1$ the regime of the antiferromagnetic phases goes to zero temperature, while for $R > \frac{1}{2}$ the superantiferromagnetic phase exists also for $H < H_1$. The order-disorder transition associated with this phase seems to have non-Ising critical exponents which vary as a function of $R$ and $H$. Estimates for the exponents lead us to suggest that Suzuki's "weak universality" is valid. The behavior of the model at $T=0$ is related to known results on hard-core lattice gases. It is shown that it is useful to interpret the transitions at $T=0$ as generalized percolation transitions. Since the model may have applications to adsorbate phases in registered structures at (100) surfaces of cubic crystals, the transcription of our results to temperature-coverage phase diagrams and adsorption isotherms is discussed in detail, and possible experimental applications are mentioned.

## I. INTRODUCTION

The Ising square lattice with nearest-neighbor (NN) coupling is one of the few exactly soluble models which shows a phase transition.[1-3] Adding next-nearest-neighbor (NNN) interactions or a magnetic field (or both) to the model, in which case it is no longer soluble, is not just an exercise of statistical mechanics: on the one hand, several layered crystals have been found which are quasi-two-dimensional anisotropic antiferromagnets (like $K_2CoF_4$, $Rb_2CoF_4$, etc.)[4-6] which can be represented by Ising models at least within a fair approximation. Since, as we shall see, the existence of NNN interactions and the magnetic field may give rise to other phases with different critical behavior, multicritical points, etc., the investigation of this more complicated model could be a valuable guideline for the analysis of corresponding experiments. On the other hand, this system can also be considered as a model for an adsorbed monolayer on a cubic (100) surface (where adsorbate atoms are only allowed to occupy "preferred sites" at the substrate surface).[7] In fact, this model has been suggested to explain some properties of H on W (100) (Ref. 8) and Te on Cu (001),[7,9] and related models on other lattices are discussed in connection with O on W (110),[10-13] with He on graphite,[14-17] etc. And last but not least, this model is a very suitable testing ground for various concepts on order-parameter symmetry[18,19] as well as for approximate methods for calculating phase diagrams, e.g., mean-field approximations[20,21] and variants thereof, real-space renormalization-group techniques,[22-24] approximate interface free-energy calculations,[25,26] series expansions,[27] many-fermion theory,[28] etc.

In the present work we present a detailed numeri-

 

cal investigation of this model, using standard Monte Carlo methods.[29] Since some aspects of the zero-field case using this technique are described elsewhere,[30] we concentrate here on the case of nonzero fields,[31] discussing the resulting phase diagrams both of the magnetic models and of the adsorbate layer models. The outline of our paper is as follows: In Sec. II, we define the model and the quantities which are computed, summarize the transcription from the Ising magnet to the adsorbed layer. We then investigate the ground-state properties of the model, with emphasis on percolationlike phenomena and the relation to hard-core lattice gases.[32] In Sec. III we shall describe the treatment of the model using a four-sublattice mean-field treatment. In Sec. IV we shall present quite detailed Monte Carlo results for the case of nearest-neighbor interaction only, while in Sec. V we shall describe the phase diagrams and thermodynamic behavior obtained for nonzero (NNN) interaction. In Sec. VI we shall consider the critical and crossover behavior exhibited by this model. Conclusions are presented in Sec. VII.

## II. THE MODEL: DEFINITIONS, ANALOGIES, AND GROUND-STATE PROPERTIES

### A. Definitions and analogies

We consider the Hamiltonian of a two-dimensional magnet

$$\mathcal{H} = -J_{\mathrm{NN}} \sum_{\mathrm{NN}} \sigma_i \sigma_j - J_{\mathrm{NNN}} \sum_{\mathrm{NNN}} \sigma_i \sigma_k - H \sum_i \sigma_i \ , \tag{1}$$

where $\sigma_i, \sigma_j, \sigma_k = \pm 1$, $J_{\mathrm{NN}}$ and $J_{\mathrm{NNN}}$ are NN- and NNN-exchange constants, respectively, $H$ is a uniform magnetic field (measured in units of the magnetic moment per magnetic ion), and the sums run over the indicated pairs of neighbors on the square lattice. For the Monte Carlo calculation, a finite $L \times L$ lattice with periodic boundary conditions is used (usually we take $L = 40$ except where otherwise stated). Energy $U$, specific heat $C_H$, magnetization $M$, and susceptibility $\chi_T$ (all quantities normalized per spin, where $N = L^2$) are then obtained as

$$\begin{aligned} U &= \frac{1}{N}\langle \mathcal{H} \rangle, \quad C_H = \frac{1}{N k_B T^2}\left(\langle \mathcal{H}^2 \rangle - \langle \mathcal{H} \rangle^2\right) \ , \\ M &= \frac{1}{N}\sum_i \langle \sigma_i \rangle \ , \\ \chi_T &= \frac{1}{N k_B T}\left[\left\langle \left[\sum_i \sigma_i\right]^2 \right\rangle - \left\langle \sum_i \sigma_i \right\rangle^2\right] \ . \end{aligned} \tag{2}$$

Since we want to analyze the system with respect to various orderings, we divide our lattice into four sublattices: 1, 2, 3, 4 (appropriate for the description of an arbitrary superstructure with twice the lattice spacing of the original lattice). In terms of the sublattice magnetizations

$$M_\lambda = \frac{4}{N}\sum_{i \in \lambda} \langle \sigma_i \rangle, \quad \lambda = 1,2,3,4 \ , \tag{3}$$

where the corners of a simple square are labeled counter-clockwise to indicate the sublattices, we obtain the order parameter of the antiferromagnetic (AF) structure

$$M_{\mathrm{AF}} = [M_1 + M_3 - (M_2 + M_4)]/4 \ . \tag{4}$$

The order parameter of the superantiferromagnetic (SAF) structure, where rows of up spins and rows of down spins parallel to the [10] or [01] direction on the lattice alternate, has two components,[18] which we write as

$$\begin{aligned} M_{\mathrm{SAF}}^{(1)} &= [M_1 + M_2 - (M_3 + M_4)]/4 \ , \\ M_{\mathrm{SAF}}^{(2)} &= [M_1 + M_4 - (M_2 + M_3)]/4 \ . \end{aligned} \tag{5}$$

As is convenient for simulations of other more-component models ($xy$ model, Heisenberg model, etc.),[29] one may introduce a root-mean-square (rms) order parameter also in this case,

$$M_{\mathrm{SAF}}^{\mathrm{rms}} = [(M_{\mathrm{SAF}}^{(1)})^2 + (M_{\mathrm{SAF}}^{(2)})^2]^{1/2} \ . \tag{6}$$

Clearly, with four sublattices there is still one more structure possible where three spins of the unit cell have the same direction, while one is pointing opposite.[7,21] The four components of this structure are

$$\begin{aligned} M_{\mathrm{IV}}^{(1)} &= (M_1 + M_2 + M_3 - M_4)/4 \ , \\ M_{\mathrm{IV}}^{(2)} &= (M_2 + M_3 + M_4 - M_1)/4 \ , \\ M_{\mathrm{IV}}^{(3)} &= (M_3 + M_4 + M_1 - M_2)/4 \ , \\ M_{\mathrm{IV}}^{(4)} &= (M_4 + M_1 + M_2 - M_3)/4 \ , \end{aligned} \tag{7}$$

and the corresponding root-mean-square order parameter is

$$M_{\mathrm{IV}}^{\mathrm{rms}} = \left[\sum_{\lambda=1}^{4} (M_{\mathrm{IV}}^{(\lambda)})^2\right]^{1/2} \ . \tag{8}$$

Since $M = \frac{1}{4}(M_1 + M_2 + M_3 + M_4)$, the $2^4/2 = 8$ order-parameter coordinates possible with four sublattices are thus exhausted (the factor 2 in the denominator accounts for changing the sign of the order parameters). However, since no general theorem restricts the number of sublattices for ordered structures in our case, one should allow for magnetic superstructures with larger elementary cells as well, and analyze the spin configurations with respect to that orderings. We did not do this but restricted ourselves to frequent, careful, visual inspection of printed-out spin configurations, which never gave any indication that any ordering with periodicity

larger than $(2\times 2)$ was present *at nonzero temperatures*. Hence the superstructures with considerably larger periodicity familiar from the adsorbate layer studies on transition metals[33,34] presumably have to be attributed to a longer range of interaction—which would not be surprising because the indirect interaction via both substrate conduction electron scattering[35] and via elastic distortion of the substrate surface[36] are of long range.

Among the susceptibilities conjugate to our various order parameters, we have only obtained the staggered (antiferromagnetic) susceptibilities $\chi_{\rm AF}$, $\chi^+$

$$\chi^+=\frac{1}{Nk_BT}\langle(M_{\rm SAF}^{\rm rms})^2\rangle \ ,$$

$$\chi_{\rm AF}=\frac{1}{Nk_BT}\left[\left\langle\left(\sum_{i\in 1}\sigma_i+\sum_{i\in 3}\sigma_i-\sum_{i\in 2}\sigma_i-\sum_{i\in 4}\sigma_i\right)^2\right\rangle - (NM_{\rm AF})^2\right] \ . \tag{9}$$

As is well known, the ordering susceptibilities can in principle be measured from diffuse magnetic neutron scattering intensities at those positions in reciprocal space where in the ordered-phase Bragg peaks (with intensity proportional to the square of the respective order parameter) occur.

Next we discuss the relation to the adsorption problem. Assume that a binding energy $\epsilon$ is won if an adsorbate occupies one of the preferred sites on the substrate surface which are assumed to form a square lattice. With an occupation variable $c_i=(0,1)$, for each site the coverage $\theta$ is

$$\theta=\frac{1}{N}\sum_i\langle c_i\rangle \ . \tag{10}$$

In terms of the adatom-adatom interaction $\phi$, the Hamiltonian can be written as

$$\mathcal{H}-\mu N_a=-\tfrac{1}{2}\sum_{i,j}c_ic_j\phi(\vec{r}_i-\vec{r}_j) - (\epsilon+\mu)\sum_i c_i+\mathcal{H}_0 \ , \tag{11}$$

where $\mu$ is the chemical potential, $N_a$ is the number of adsorbed atoms, and $\mathcal{H}_0$ describes other degrees of freedom (vibrations etc.). With $c_i=\frac{1}{2}(1-\sigma_i)$, we transform to the equivalent Ising model of a magnet

$$\mathcal{H}=-\tfrac{1}{2}\sum_{i,j}J(\vec{r}_i-\vec{r}_j)\sigma_i\sigma_j-H\sum_i\sigma_i+\mathcal{H}_0' \ , \tag{12}$$

where

$$J=\phi/4, \quad H=-\left(\epsilon+\mu+\tfrac{1}{2}\sum_j\phi\right)\Big/2 \ . \tag{13}$$

Note that this transcription is identical to the usual lattice-gas Ising-magnet analogy[37] apart from the fact that the binding energy per site $\epsilon$ has been added to the chemical potential. As is well known, a treatment of the Ising magnet in the canonic ensemble corresponds to a treatment of the lattice gas in the grand canonic ensemble. Equation (12) reduces to Eq. (1), of course, if the background term $\mathcal{H}_0'$ which is of no interest here is omitted, and $J(\vec{r}_i-\vec{r}_j)$ is taken to be nonzero only if $\vec{r}_i-\vec{r}_j$ equals a lattice vector between NN or NNN.

The magnetization process $M=M(H,T)$ of the Ising magnet corresponds to the adsorption isotherm $\mu=\mu(\theta,T)$ of the (physisorbed) monolayer, since

$$\frac{\mu}{k_BT}=\frac{1}{Nk_BT}\left(\frac{\partial F}{\partial\theta}\right)_T=-\frac{2H}{k_BT}+\frac{\mu_c}{k_BT} \ , \tag{14}$$

where $F$ is the free energy,

$$\mu_c=-\epsilon-\tfrac{1}{2}\sum_j\phi(\vec{r}_j-\vec{r}_j) \ , \tag{15}$$

and

$$\theta=(1-M)/2 \ . \tag{16}$$

Note that $\mu/k_BT$ is proportional to the logarithm of the adsorbate gas pressure if the gas is assumed to be ideal. For pairwise interactions, the phase diagram in the $(T,\theta)$ plane is symmetric around $\theta_c=\frac{1}{2}$, while the adsorption isotherms are antisymmetric around the point $(\theta_c=\frac{1}{2},\ \mu=\mu_c)$. But the maximum coverage even at $T=0$ is given by $\theta_{\rm max}=1$ only if $\mu_c<0$, while otherwise only the part of the phase diagram for which $\mu\leq 0$ can be realized. This lattice gas with pairwise interaction is a poor model for real adsorbate systems at larger coverages due to many-body interactions and multilayer adsorption,[38] however.

### B. Ground-state properties

We first consider the ground state in the magnetic case. For $J_{\rm NN}>0$ (ferromagnetic), $R\equiv J_{\rm NNN}/J_{\rm NN}>0$ the ground state is ferromagnetic for arbitrary fields. For $J_{\rm NN}>0$, $R<0$ the ground state is superantiferromagnetic if $2J_{\rm NN}(1+2R)<-H$, which is possible only for $R<-\frac{1}{2}$. In this case, the superantiferromagnetic state is the ground state in zero field, and at $H_{c1}=-2J_{\rm NN}(1+2R)$ a transition to the ferromagnetic state takes place.

For $J_{\rm NN}<0$, $R\leq 0$ the antiferromagnetic state is stable if $4J_{\rm NN}<-H$. At $H_{c2}=-4J_{\rm NN}$ a transition to the ferromagnetic state takes place. For $J_{\rm NN}<0$, $R>0$ the behavior is more difficult. The antiferromagnetic state is stable for $4J_{\rm NN}(1-R)<-H$, provided $R\leq\frac{1}{2}$. At $H_{c3}=-4J_{\rm NN}(1-R)$ a transition takes place to a degenerate structure, where ferromagnetic rows alternate with antiferromagnetic ones. The antiferromagnetic rows are not ordered with respect to each other. If they were, due to a third-neighbor attraction perhaps, the state would be

$(2\times2)$. In the present case, the $(2\times2)$ structure is degenerate with this more general $(2\times1)$ structure. The physically relevant structure to consider is the *most probable structure,*[39–41] which is the latter. (Its ground-state degeneracy is $4\times2^{L/2}$, because there are $\frac{1}{2}L$ antiferromagnetic rows, and an additional factor 2 arises from interchanging the ferro- and antiferromagnetic sublattices, and another factor 2 arises from interchanging $x,y$ directions on the square lattice.) The antiferromagnetic sublattice exhibits long-range order in one dimension only, while the ferromagnetic sublattice has true two-dimensional long-range order. This different dimensionality of the ordering at different sublattices gives rise to interesting effects at nonzero temperatures. [We have described this structure in detail because previous work[42–44] erroneously described this structure as the fully periodic four-sublattice structure of Eq. (7). In fact, if one uses the usual method[45] of constructing all possible spin arrangement of $(l\times m)$ superlattice unit cells for various values of $l,m$ to find the lowest energy state, one would have to use $l=m=4$ to just *note* that there is a degeneracy higher by a factor of 2 than expected. Also the methods where inequalities are used proving that no lower-lying states exist[46] are of little help for the degeneracy problem.] This degenerate structure now is stable for $H_{c3}<H<H_{c4}=-4J_{NN}(1+R)$, while for $H>H_{c4}$ again the ferromagnetic structure results.

In the case finally where $J_{NN}<0$ but $R\geq\frac{1}{2}$ the superantiferromagnetic structure is stable for $H<H_{c5}=-4J_{NN}R$. For $R=\frac{1}{2}$, of course, AF and SAF structures are then degenerate (and $H_{c3}=H_{c5}$ in this case). For $H>H_{c5}$, one then obtains the same degenerate structure as before, with transition to the ferromagnetic state at the above $H_{c4}$.

### C. Equivalent lattice-gas structures

The seemingly trivial transcription from Eq. (11) to Eq. (12) has rather nontrivial consequences, since now we use the coverage (corresponding to magnetization) rather than the chemical potential (corresponding to the field) as independent variable. Since in the above case the magnetization is zero in the AF and SAF structures, $\pm\frac{1}{2}$, in the degenerate structure, and $\pm1$ in the ferromagnetic structure, one has magnetization jumps at the various critical fields $H_{c1},\ldots,H_{c5}$. However, for the lattice-gas problem it makes sense to consider coverages $\theta$ different from 0, $\frac{1}{4}$, $\frac{1}{2}$, $\frac{3}{4}$, 1 [corresponding to the above magnetizations, see Eq. (16)] also in the ground state $T=0$.

We first consider the case of rather low coverages and repulsive interactions between both nearest and next-nearest neighbors. For $\theta\leq\frac{1}{4}$, the ground-state energy is always zero and entropy determines the structure. For $\theta=\frac{1}{4}$, we have the degenerate structure [Fig. 1(a)] which corresponds to the degenerate magnetic structure described above: empty rows alternate with half-filled rows (in which filled and empty sites alternate). As $\theta$ is decreased, the most probable state is given by the same structure but with imperfect order: e.g., a fraction $(1-4\theta)$ of the filled sites in Fig. 1(a) is now also empty, one thus has "clusters" of holes in the ordered structure. Inside these holes finite clusters of the ordered structure may occur, etc. Below the percolation threshold $\theta_1^*$ the infinite network of the ordered structure breaks up, and only finite clusters of the ordered structure remain. Thus the lattice-gas phase can exist in the

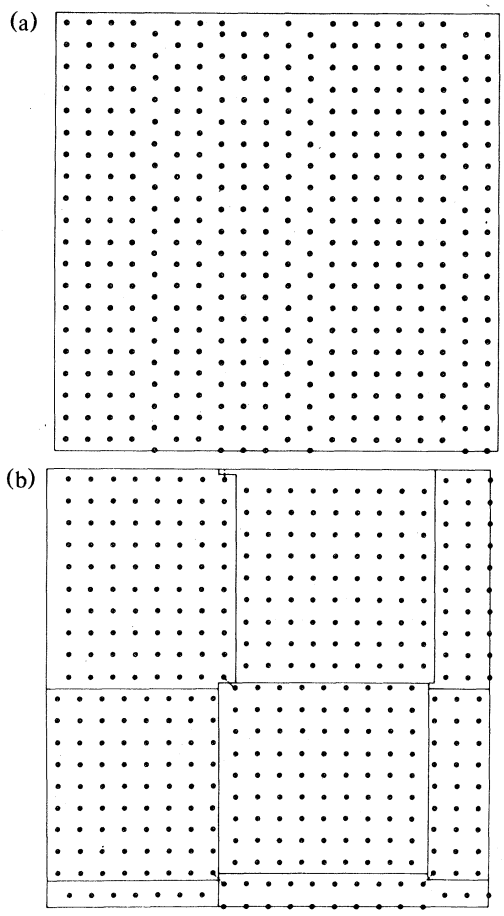


FIG. 1. (a) Typical ground-state arrangement of the degenerate structure at $\theta=\frac{1}{4}$ at a $40\times40$ square lattice with periodic boundary conditions. Filled sites are shown by black dots while empty sites are not shown. (b) Metastable domain configuration reached by slowly cooling the system from a disordered arrangement to zero temperature. Thin full lines indicate antiphase domain boundaries, while broken lines indicate "broken bonds" which cost energy.

ground state for a finite regime of "densities" (i.e., coverages in the range $0 \leq \theta \leq \theta_1^*$). Since a two-dimensional lattice for obvious geometrical reasons cannot carry two percolating networks at the same time, there is no regime of coverages where both an infinite net of the degenerate structure and an infinite net of lattice gas coexist, and we expect a second-order transition from the lattice-gas phase to the degenerate structure at $\theta_1^*$. Clearly, this is a kind of percolation problem which may be visualized as the random filling of sites with larger objects which block both nearest- and next-nearest-neighbor sites from further occupation, and where an object belongs to a "cluster" when at least one other object belonging to that cluster is either a distance $2a$ or $(5a)^{1/2}$ apart, where $a$ is the lattice spacing. This ambiguity in the cluster definition reflects the degeneracy of the ordered structure within the clusters [Fig. 1(a)]. Figure 2 shows a series of typical configurations obtained by this prescription and the resulting largest cluster on the periodic $40 \times 40$ lattice is indicated. It turns out that "percolation" occurs roughly at $\theta_1^* \approx 0.135$. This estimate for the percolation coverage is affected by the finite size of our lattice, of course; for a $25 \times 25$ lattice, the corresponding estimate was $\theta_1^* \approx 0.127$, for $55 \times 55$ at $\theta_1^* \approx 0.140$, and for $95 \times 95$ at $\theta_1^* \simeq 0.147$. Extrapolating these value to the thermodynamic limit, we obtain $\theta_1^* \approx 0.155$ as a tentative estimate. This value is in fact very close to the estimate which would be obtained by only considering the sites of one particular realization of the ordered structure [e.g., Fig.1(a)] available for occupation: Then the percolation coverage would be $\theta_1^* = p_c^{sq}/4 \approx 0.1475$, where $p_c^{sq} \approx 0.59$ is the ordinary site percolation threshold of the square lattice.[47] Hence the percolation threshold in our case seems to be only little affected by the degeneracy of the fully ordered structure.

Now we note that these ground-state properties of our system may be interpreted in an alternative way:

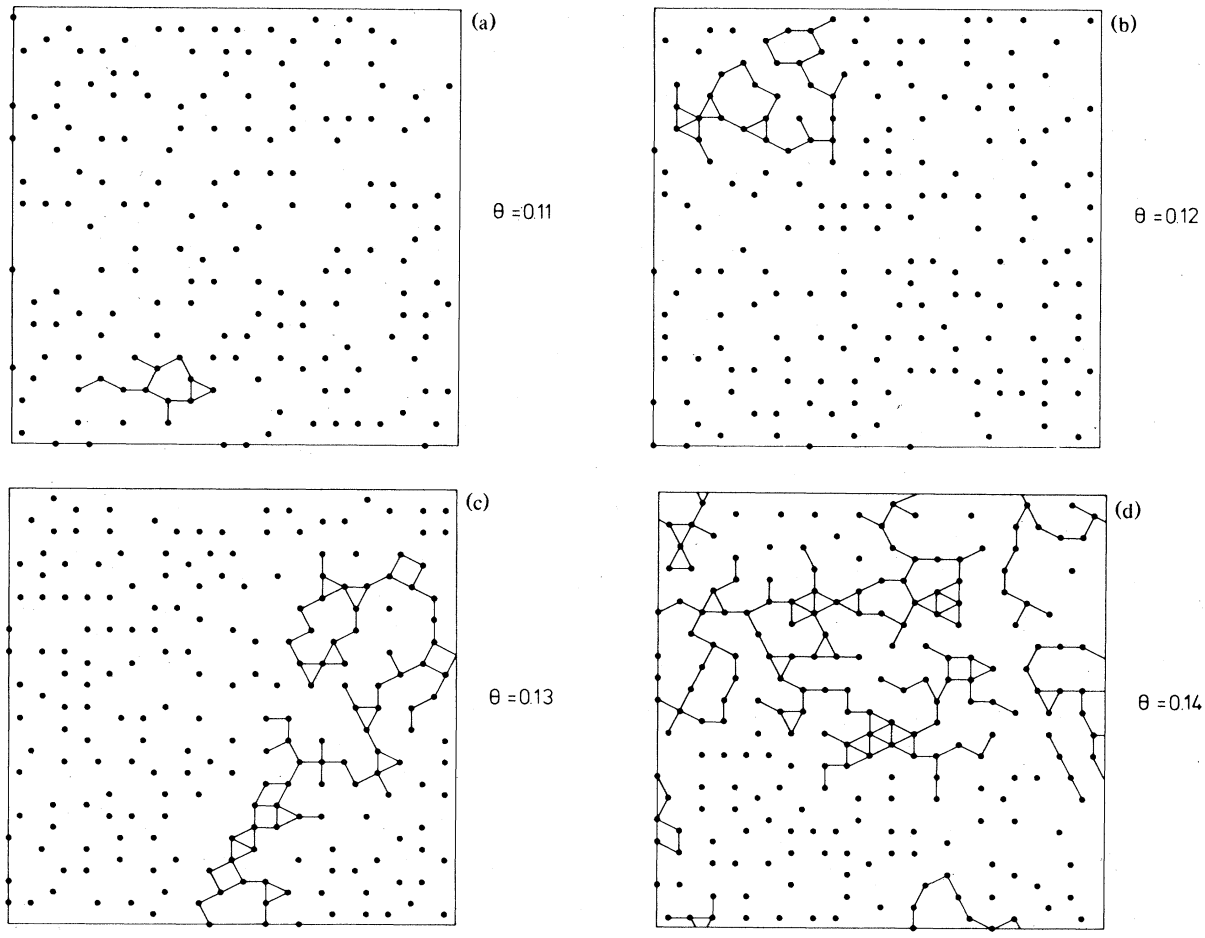


FIG. 2. Typical ground-state arrangments of a $40 \times 40$ square lattice at $\theta = 0.11$ (a), $\theta = 0.12$ (b), $\theta = 0.13$ (c), and $\theta = 0.14$ (d). The largest occurring cluster of the degenerate structure is indicated in each case.

rather than keeping the interactions $\phi_{NN}$, $\phi_{NNN}$ finite and let the temperature $T$ go to zero, one may keep $T$ finite and nonzero and one instead considers the limit $|\phi_{NN}| \to \infty$, $|\phi_{NNN}| \to \infty$. The results are then independent of the magnitude of $R$ as long as $R > 0$. The resulting system is interpreted as a hard-core lattice gas.[48–51] While from Eq. (15) it is obvious that $\mu_c/k_BT \to \infty$ in that limit, it is clear that the adsorption isotherm $\mu(\theta,T)$ is still well defined. As is well known,[48], $\mu/k_BT$ is in this case a function of coverage only,

$$\mu/k_BT = f(\theta) \ , \tag{17}$$

i.e., the dependence on temperature is trivial, if one treats the kinetic energy of the lattice gas by classical and not by quantum statistics. It is then interesting to ask whether the percolation transition at $\theta_1^*$ corresponds to any singularity of the equation of state, Eq. (17): e.g., for a thermodyamic second-order transition one would expect that the compressibility of the lattice gas diverges, and hence

$$\chi^{-1} = \left(\frac{\partial \mu}{\partial \theta}\right)_T = k_BT \frac{df(\theta)}{d\theta}\bigg|_{\theta_1^*} = 0 \ . \tag{18}$$

It is not completely clear, however, if such a transition actually occurs for $\theta_1^*$.[48] While a closed-form approximation[51] yielded a transition for $\theta_1^* \approx 0.20$, matrix methods[49,50] suggested a higher-order transition for $\theta_1^* \approx 0.2375$, while low- and high-density series expansions[50] indicated no transition. These findings contradict each other and none of the estimates for $\theta_1^*$, agrees with our estimate. Hence more work is necessary to resolve this problem. In view of this uncertainty in the location of $\theta_1^*$, we did not attempt to determine any critical exponents for this transition. While in some of the early series-expansion studies[52] on hard-core lattice gases it was suggested that the exponents are the same as that of the ordinary lattice gas [i.e., nonordering susceptibility at $H \neq 0$ $\propto (\theta_1^* - \theta)^{-\alpha} \propto |\log(\theta_1^* - \theta)|$ since $\alpha = 0$, order parameter $\propto (\theta - \theta_1^*)^{1/8}$ in two dimensions], we rather suggest that the exponents belong to a class of percolation problems [in the ordinary site-percolation problem we would have order parameter $\propto (\theta - \theta_1^*)^{\beta_p}$, susceptiblity $\propto (\theta_1^* - \theta)^{-\gamma_p}$ with[53] $\gamma_p = 2.2$, $\beta_p = 0.139$, but here the situation is different since it is the difference in occupation of the sublattices which matters for the order parameter].

For $\theta > \frac{1}{4}$ and $R > 0$ the ground-state energy of our model is no longer zero, but rather is given by ($E_G$ is the ground-state energy per particle)

$$E_G = -(4\theta - 1)\phi_{NNN}, \quad R \leq \tfrac{1}{2} \ , \tag{19a}$$

$$E_G = -\tfrac{1}{2}(4\theta - 1)\phi_{NN}, \quad R \geq \tfrac{1}{2} \ . \tag{19b}$$

Although the energy now is no longer zero, the degeneracy of the ground state is still very high. Suppose we would start from a $2 \times 2$ structure with $\theta = \frac{1}{4}$, sublattice 1 being filled: then in case of Eq. (19a) the sites of sublattice 3 could be filled at random with probability $4\theta - 1$, while in case of Eq. (19b) the sites of either sublattice 2 or sublattice 4 are filled. One then asks for the concentration $\theta_2^*$ at which for the first time an infinite network of $c(2 \times 2)$ structure [in case of Eq. (19a)] or $2 \times 1$ structure [in case of Eq. (19b)] appears. Obviously, this happens at the percolation threshold $p_c^{sq}$ of the respective sublattice, and hence the resulting estimate for $\theta_2^*$ is $\theta_2^* = \frac{1}{4} + p_c^{sq}/4 \cong 0.3975$. This estimate is not very accurate, of course, since starting from a $(2 \times 2)$ structure [or starting from the structure of Fig. 1(a)] introduces a bias in the sampling of ground-state configurations. In order to obtain an unbiased estimate, we employed the following procedure: in the case of Eq. (19a), we filled the lattice sites successively at random with the constraint that no neighboring sites were occupied. Since the resulting structures have energies exceeding $E_G$, in a second step the energy of the structure was minimized by randomly repositioning particles from filled sites if this lowered the energy. Simultaneous rearrangments of two particles were also considered. These rearrangements were sufficient to come quite close to $E_G$ for $\theta$ close to $\theta_2^*$. Figure 3 shows a set of typical arrangments obtained in this way. One observes ramified clusters, the typical size of which strongly increases as $\theta_2^*$ is reached. Our estimate for the percolation concentration on a $40 \times 40$ lattice is $\theta_2^* \approx 0.365$, while the tentative estimate for the percolation concentration in the thermodynamic limit, again based on extrapolating estimates for lattices of various sizes, is $\theta_2^* \approx 0.38$. While these data seem to indicate that the order parameter of the $c(2 \times 2)$ structure increases with $\theta \geq \theta_2^*$ in a continuous way, appropriate for a second-order transition, it is much harder to ascertain that the order parameter of the degenerate structure vanishes continuously for $\theta \to \theta_2^*$ from below. Thus it is conceivable that the transition from the degenerate structure to the $c(2 \times 2)$ structure (or $2 \times 1$ structure, respectively) is of first order, implying the existence of a mixed-phase regime of coverages in the vicinity of $\theta_2^*$. Our data at nonzero temperatures, however, are consistent with the conjecture that the transition stays second order throughout to $T = 0$.

Again this percolation transition can be interpreted in terms of hard-core lattice gases, with a "soft core" (finite next-nearest-neighbors repulsion energy) added to the nearest-neighbor hard core, in the limit $T \to 0$. But so far this model has been studied for nonzero temperatures only.[54]

A much simpler situation arises for $R = 0$. Then the ground state of the system is found by the re-

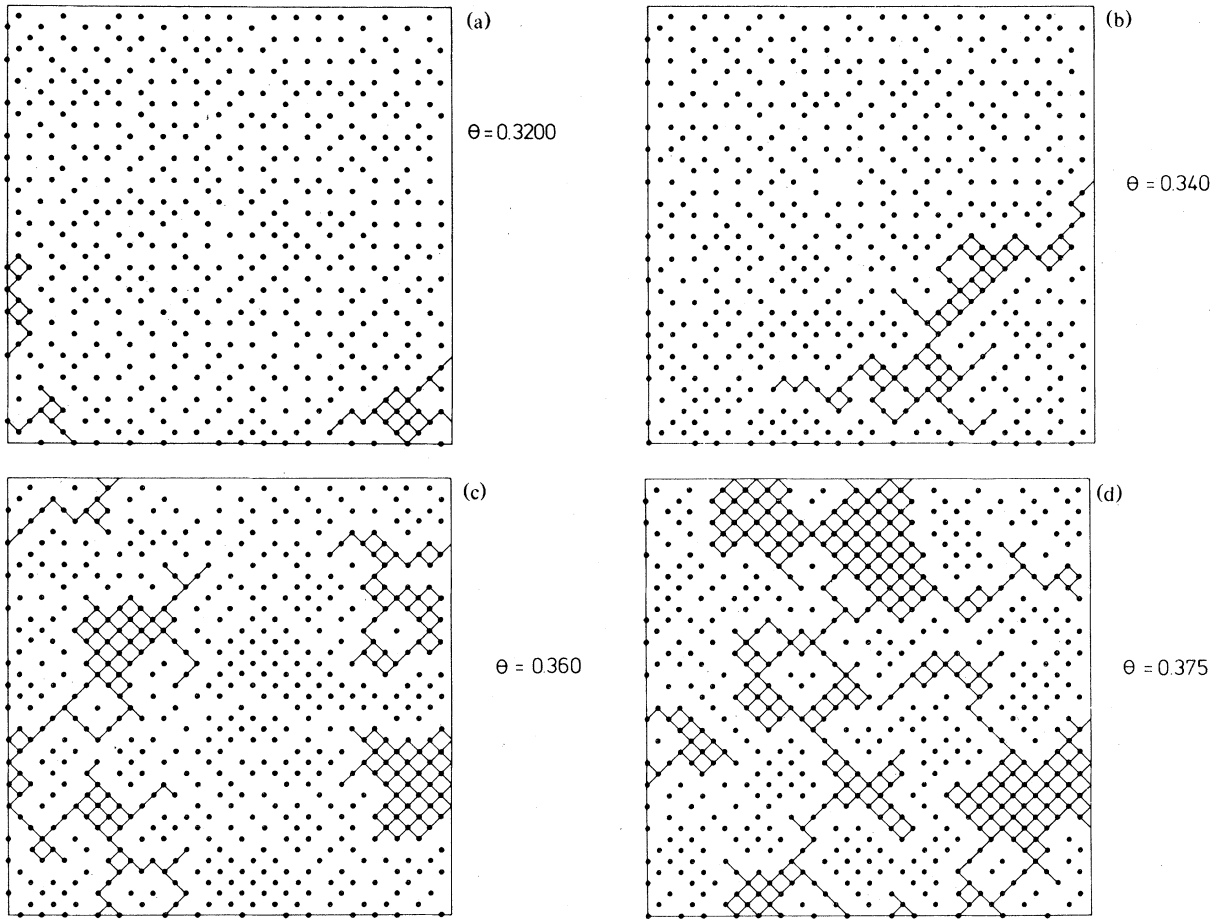


FIG. 3. Typical ground-state arrangments of a $40 \times 40$ square lattice with $0 < R < \frac{1}{2}$ at $\theta = 0.320$ (a), $\theta = 0.340$ (b), $\theta = 0.360$ (c), and $\theta = 0.375$ (d). The largest occurring cluster of the $c(2 \times 2)$ structure is indicated in each case.

striction that no nearest-neighbor pairs occur, but otherwise the lattice may be filled at random. One now asks for the percolation threshold $\theta^*$ at which an infinite net of the $c(2 \times 2)$ structure occurs. While for a $40 \times 40$ lattice our estimate is $\theta^* \approx 0.36$, the tentative estimate obtained via extrapolation to the infinite system is $\theta^* \approx 0.375$. We hence find only insignificant differences to the values for $\theta_2^*$ obtained above. Furthermore we note excellent agreement with the coverage $\theta^* = 0.371$ (Ref. 48) at which the transition in the equivalent hard-core lattice gas with nearest-neighbor exclusion occurs. Again we suggest that the exponents describing this transition are those of the percolation problem rather than those of the ordinary Ising model.

No such percolationlike phenomena occur if some interactions are attractive, of course. For example, for $\phi_{NN}$ repulsive and $R < 0$ it is energetically favorable to form a domain of perfect $c(2 \times 2)$ structure (coverage $\theta = \frac{1}{2}$) coexisting with lattice gas (coverage $\theta = 0$) for all $0 < \theta < \frac{1}{2}$ according to the lever rule. If also $\phi_{NN}$ is attractive, rather, domains of high-density lattice gas ($\theta = 1$) and low-density lattice gas ($\theta = 0$) coexist.

## III. MEAN-FIELD TREATMENT

In order to consider models such as Eq. (1) (on general lattices) using mean-field theory, we decompose the lattice under consideration into $\nu$ sublattices $\{\alpha\}$ which are subject to fields $\{H_\alpha\}$ which act on the sites of the $\alpha$th sublattice only. The ordinary magnetic field is then given by

$$H = \frac{1}{\nu} \sum_{\alpha=1}^{\nu} H_\alpha \tag{20}$$

and other linear combinations of these fields constitute the various possible "staggered fields". [In a simple two-sublattice antiferromagnetic, $\nu = 2$, and

there is only one other linearly independent combination of $H_1, H_2$, namely, the ordinary staggered field $H^+ = \frac{1}{2}(H_1 - H_2)$.] In order to introduce the mean-field approximation, we separate the interaction term into sublattice contributions and rewrite the Hamiltonian as

$$\mathcal{H} = \sum_{\alpha=1}^{\nu} \sum_{i \in \alpha} H_\alpha^{\text{eff}}(\{\sigma_j\})\sigma \quad , \tag{21}$$

where

$$H^{\text{eff}}(\{\sigma_j\}) = H_\alpha + \sum_{\beta=1}^{\nu} \sum_{j \in \beta} J_{ij}\sigma_j, \quad i \in \alpha \quad . \tag{22}$$

We then replace $H_\alpha^{\text{eff}}$ by its average value,

$$\bar{H}_\alpha^{\text{eff}} = H_\alpha + \sum_{\beta=1}^{\nu} \sum_{j \in \beta} J_{ij}\langle \sigma_j \rangle \quad , \tag{23a}$$

$$= H_\alpha + \sum_{\beta=1}^{\nu} \epsilon_{\alpha\beta} m_\beta \quad , \tag{23b}$$

where we have defined a sublattice magnetization

$$m_\beta = \frac{\nu}{N} \sum_{j \in \beta} \langle \sigma_j \rangle \tag{24}$$

and an interaction parameter

$$\epsilon_{\alpha\beta} = \sum_{j(\neq i)} J_{ij}, \quad i \in \alpha, \quad j \in \beta \quad . \tag{25}$$

The mean-field Hamiltonian then becomes

$$\mathcal{H}^{\text{MFT}} = \sum_{\alpha=1}^{\nu} \sum_{i \in \alpha} \left( \sum_{\beta=1}^{\nu} \epsilon_{\alpha\beta} m_\beta + H_\alpha \right) \sigma_i - \frac{1}{2} \sum_{\alpha=1}^{\nu} \frac{N}{\nu} \sum_{\beta=1}^{\nu} \epsilon_{\alpha\beta} m_\alpha m_\beta \quad , \tag{26}$$

where the second term corrects for overcounting, as usual. It is straightforward to show that the free energy is given by

$$F^{\text{MFT}} = -k_B T \ln 2 - \frac{k_B T}{\nu} \sum_{\alpha=1}^{\nu} \ln \cosh \left[ \frac{1}{k_B T} \left( \sum_{\beta=1}^{\nu} \epsilon_{\alpha\beta} m_\beta + H_\alpha \right) \right] + \frac{1}{2\nu} \sum_{\alpha=1}^{\nu} \sum_{\beta=1}^{\nu} \epsilon_{\alpha\beta} m_\alpha m_\beta \quad . \tag{27}$$

The sublattice magnetizations are related to the free energy by

$$m_\alpha = -\nu \left( \frac{\partial F}{\partial H_\alpha} \right)_{T, H_{\beta \neq \alpha}}, \quad \alpha = 1, \ldots, \nu \quad , \tag{28}$$

and from Eq. (27) we find, as expected,

$$m_\alpha = \tanh \left[ \frac{1}{k_B T} \left( \sum_{\beta=1}^{\nu} \epsilon_{\alpha\beta} m_\beta + H_\alpha \right) \right] \quad , \tag{29}$$

$$\alpha = 1, \ldots, \nu \quad .$$

Usually the solutions of Eq. (29) will not be unique (i.e., several ordered structures are possible). Using then the solutions of Eq. (29) in Eq. (27), one can find the structure for which $F^{\text{MFT}}$ is minimal, which hence is the stable structure, while the other structures are metastable or unstable ones.

Due to the nonlinear character of Eq. (29), an analytic solution of this system of coupled equations in general is not possible. Instead we used the numerical iteration procedure

$$m_\alpha^{(n)} = \cos^2\phi\, m_\alpha^{(n-1)} + \sin^2\phi \tanh \times \left[ \frac{1}{k_B T} \left( \sum_{\beta=1}^{\nu} \epsilon_{\alpha\beta} m_\beta^{(n-1)} + H_\alpha \right) \right] \quad , \tag{30}$$

$$\alpha = 1, \ldots, \nu, \quad n \geq 2 \quad ,$$

where $\phi$ is an arbitrary parameter ($0 < \phi < \frac{1}{2}\pi$), which must be chosen so that Eq. (30) is actually convergent, i.e., so that

$$\lim_{n \to \infty} |m_\alpha^{(n)} - m_\alpha^{(n-1)}| = 0, \quad \alpha = 1, \ldots, \nu \quad . \tag{31}$$

The best choice of $\phi$ is related to the choice of an initial condition $\{m_\alpha^{(1)}\}$ for the iteration, and this in turn may depend upon the number and possible arrangement of the sublattices. If one begins with a saturated (anti-) ferromagnet, $\{m_\alpha^{(1)} = \pm 1, \alpha = 1, \ldots, \nu\}$, it turns out that the choice $\phi = \frac{1}{2}\pi$, which would give the quickest possible convergence, very frequently leads to oscillatory rather than convergent behavior (at least for some of the $m_\alpha$'s). In the case of the four-sublattice structure on the square lattice [Eq. (7)] with $R > 0$, the choice $\phi = \frac{1}{4}\pi$ yielded satisfactory results in most cases. It turned out that nonconvergent behavior (i.e., oscillatory or erratice "turbulent" behavior) occurred less frequently the smaller $\phi$ is chosen and the higher temperatures are investigated. Usually the convergence of Eq. (30) is quite rapid (i.e., all $m_\alpha$ are stable to five significant digits after $n > 10^2$ iterations), except if one is close to a second-order phase transition, where much larger $n$ are required. This slowing down of the convergence can be understood as critical slowing down of the kinetic Ising model. In fact, interpreting $n$ as a time $t$ and taking the limit $\phi \to 0$, Eq. (30) reduces to a set of equations similar to that derived by Suzuki and Kubo[55] for a ferromagnet, namely,

$$\frac{1}{\phi^2} \frac{dm_\alpha}{dt} = -\left\{ m_\alpha(t) - \tanh \left[ \frac{1}{k_B T} \left( \sum_{\beta=1}^{\nu} \epsilon_{\alpha\beta} m_\beta(t) + H_\alpha \right) \right] \right\}, \quad \alpha = 1, \ldots, \nu \quad . \tag{32}$$

From the analysis of the nonequilibrium relaxation of kinetic mean-field models,[56] it follows that, in the case where Eq. (29) has several solutions, one can only reach stable and metastable points using Eq. (32), but never unstable ones. In such a case of multiple solutions, thermodynamic equilibrium usually requires somewhere a first-order transition from one branch of the solutions to another. Since in the general case the hysteresis loops need not be antisymmetric around the point of unstable equilibrium, a Maxwell equal-area construction to locate the transition is in general not possible without the knowledge of the unstable branch. But first-order phase transitions can be located unambiguously by comparing the free energies of the various branches, using Eq. (27). In order that one actually locates the various possible branches, one has to repeat the iteration several times with different initial conditions. It is convenient to use all structures which are stable *somewhere* in the phase diagram as initial conditions *everywhere*. Although no guarantee can be given that all ordered phases are thus detected and their range of stability in the phase diagram located, we think that the method developed here is flexible and practically useful.

We applied this technique to the case $J_{NN} < 0$, $J_{NNN} < 0$, $H \gtrless 0$, which was previously studied by Katsura and Fujimori[21] by a less general method. Figure 4 shows our results for the phase diagram in the $H,T$ plane for $R = \frac{1}{4}$, $\frac{1}{2}$, and 1. For small $R$ the phase transition from the paramagnetic phase is always into the antiferromagnetic phase [Fig. 4(a)]. If the field is increased at low enough temperatures, one finds a transition to the four-sublattice structure of Eq. (7). At still higher fields there is a second transition back to the antiferromagnetic phase, before then finally the transition to the paramagnetic phase occurs. At larger $R$ the succession of phase transitions changes: the stability regime of the four-sublattice superstructure then extends up to the critical point of the antiferromagnetic phase in zero field, and it transforms directly into the paramagnetic phase at higher fields without going back to the antiferromagnetic phase. The transition from the four-sublattice structure to the disordered phase seems to be second order. But now the transition from the antiferromagnetic phase to the four-sublattice structure is of first order. For $R = \frac{1}{2}$, the antiferromagnetic phase becomes degenerate with the superantiferromagnetic one [Fig. 4(b)]. For $R > \frac{1}{2}$, the antiferromagnetic phase is no longer stable; at low magnetic fields the superantiferromagnetic phase is stable [Fig. 4(c)], which then transforms into the four-sublattice structure at higher fields. This transition is of first order.

Most of these findings agree with those of Katsura and Fujimori[21]; but they predict the transition from

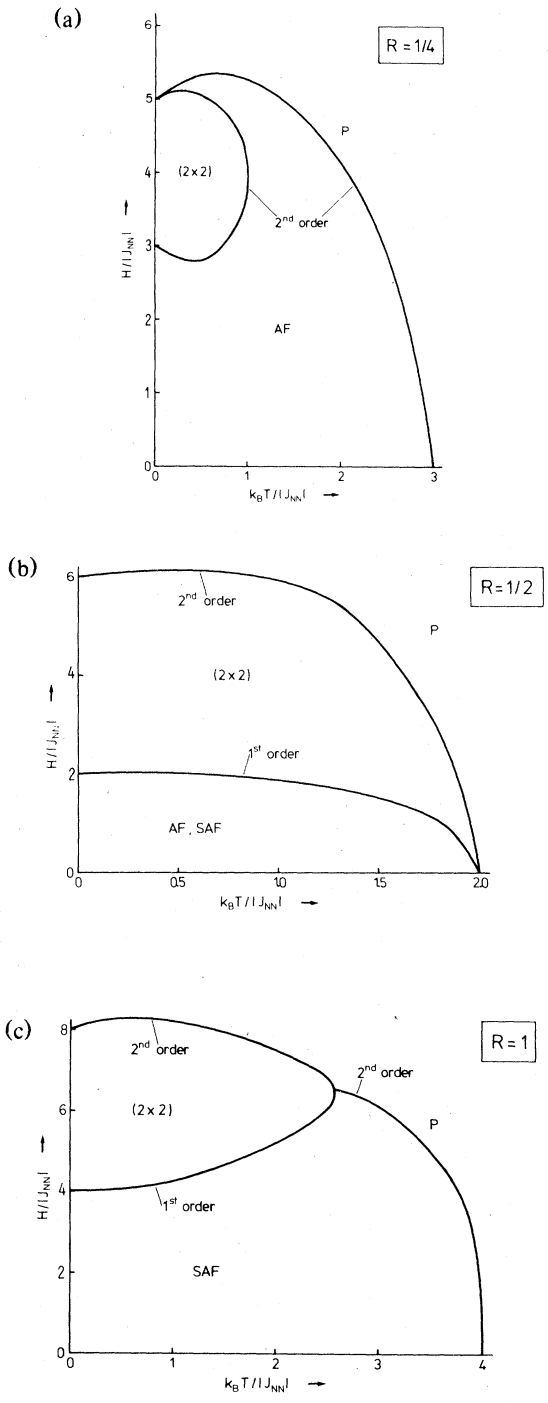


FIG. 4. Mean-field phase diagram of Ising antiferromagnets in a field for $R = J_{NNN}/J_{NN} = \frac{1}{4}$ (a), $R = \frac{1}{2}$ (b), and $R = 1$ (c). Phases occurring are paramagnetic (P), antiferromagnetic (AF), superantiferromagnetic (SAF) and the four-sublattice superstructure $(2 \times 2)$. The order of the various phase transitions is indicated.

the four-sublattice phase to the antiferromagnetic phase as the field is increased to be a first-order transition, while the transition from the antiferromagnetic phase to the four-sublattice phase is predicted to be of second order as in our calculation. Since the phase boundaries are calculated from the numerical solution of Eq. (30) an extremely small jump of first derivatives of the free energy there can never be firmly excluded. Due to the same reason Figs. 4(c) and 6(c) may be slightly inaccurate close to the multicritical point. Figure 5 shows the behavior of order parameters and free energies for a few typical cases to illustrate the type of data used for the judgement. We think that for $R=\frac{1}{4}$ the transition can be at best very weakly of first order and hence at least for all practical purposes it is sufficient to describe it as second-order transition. In the case of $R=\frac{1}{2}$, however, the free-energy curves are quite distinctly intersecting, and hence pronounced magnetization jumps occur: the transition from the AF or SAF phase to the $(2\times 2)$ structure clearly is of first order. In Ref. 21 this transition at $R=\frac{1}{2}$ was described as second order, which is excluded from the above symmetry argument.

From Fig. 5 we can recognize another remarkable feature: While the free energies of the various phases typically are of order $F\approx k_BT$, the free-energy differences often are of order $\Delta F\approx 10^{-2}k_BT$, even quite far apart from the transition. Since mean-field approximations are expected to yield $F/k_BT$ accurate to about 10% only, it is clear that the predicted transition lines are very unreliable, and it is also doubtful that the predictions for the order of the various transitions are correct. In Sec. V it will in fact be shown that most of the mean-field predictions seriously are in error.

Using our results and Eq. (16), it is easy to construct the phase diagrams in the variables temperature and coverage appropriate to the adsorbed-layer problem, Fig. 6. Due to the jumps of magnetization

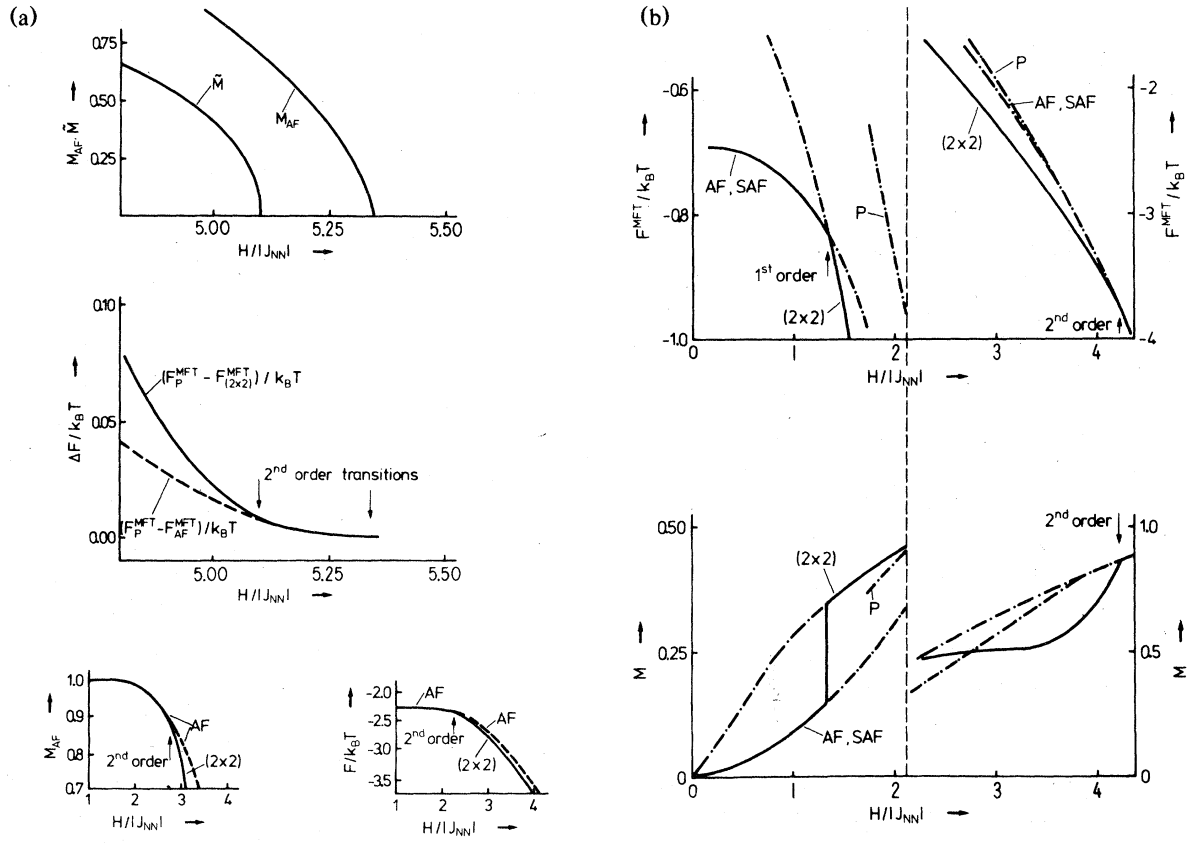


FIG. 5. (a) Mean-field results for $R=\frac{1}{4}$, $k_BT/|J_{NN}|=\frac{1}{2}$. Both the staggered magnetization $M_{AF}$, an order-parameter component of the $(2\times 2)$ structure $[\tilde{M}=\frac{1}{2}(M_1-M_3)]$, and the free-energy differences between the various phases are plotted as function of the field. (b) Mean-field results for $R=\frac{1}{2}$, $k_BT/|J_{NN}|=0.725$. Free energies and magnetization of the various phases are plotted vs magnetic field.

(coverage) at first-order phase transitions, one obtains then mixed-phase regions. Note that the mean-field approximation does not yield any nontrivial behavior of the ground states at $T=0$, of course: in order to obtain any of the percolation coverages $\theta_1^*$, $\theta_2^*$ different from zero or one-half, one would have to go beyond mean-field theory.

Figure 7 then presents our results for the adsorption isotherms, which correspond to the magnetization process of the respective Ising antiferromagnets. While first-order transitions show up by a jump, second-order transitions correspond to much weaker singularities (in this approximation jumps of the derivative of the adsorption isotherm may occur). We defer a detailed discussion of these results to Sec. V where they will be compared to the more accurate Monte Carlo data.

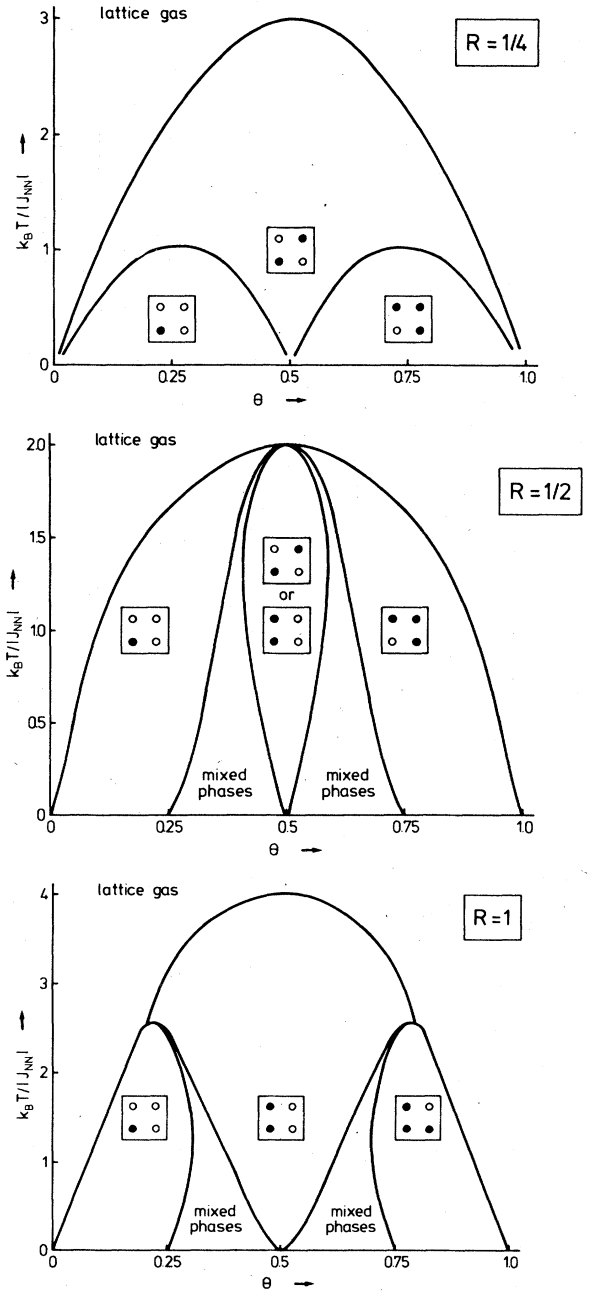


FIG. 6. Mean-field phase diagram of an adsorbed layer with repulsive nearest- and next-nearest-neighbor interactions for $R=\frac{1}{4}$, (a), $R=\frac{1}{2}$ (b), and $R=1$ (c). Elementary cells of the various occurring superstructures are indicated.

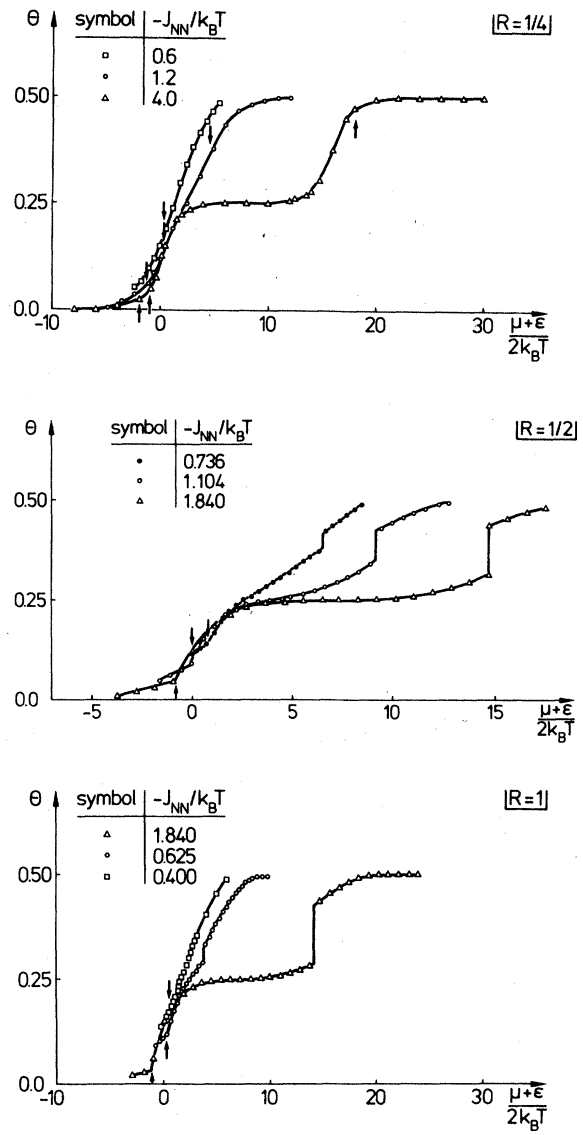


FIG. 7. Adsorption isotherms $\theta=\theta(\mu,T)$ calculated from mean-field theory for the adsorbed layers shown in Fig. 6. Arrows indicate the occurring second-order phase transitions.

## IV. RESULTS FOR $R = 0$

For the case of $R = 0$ the problem is simply that of a nearest-neighbor Ising model in a magnetic field. We are particularly interested in this case since there already exists a number of solutions obtained by clearly approximate methods,[23,24,27,57–60] as well as an interface free-energy treatment which purports to give the exact critical-field curve.[25] We took special care to acquire extensive data in this case. Finite-size effects were studied by examining $20 \times 20$, $40 \times 40$, and $80 \times 80$ lattices with observation times $t$ of 2000–4000 MCS (Monte Carlo steps) for each data point. (In addition each point was repeated at least once.) The major part of the investigation was carried out along paths of constant $H/T$. An approximate phase boundary was constructed from the locus of points of maximum slope in the magnetization results. (The error bars were much smaller than those obtained in another Monte Carlo study[61] carried out along paths of constant $H$.) The results agree well with the "interface solution"[25]; however, a much more demanding comparison may be made by invoking the universality principle and carrying out a careful analysis of the Monte Carlo order-parameter data assuming that $\beta$ retains its $H = 0$ value of $\frac{1}{8}$. The variation of the order parameter versus temperature is shown in Fig. 8(a) for several different paths of constant $H/T$. The differences between the sets of data reflect the increase in critical amplitude which occurs as the path steepens. Similarly the critical amplitude for the specific heat decreases as the path steepens. As the data in Fig. 8(b) show, the specific-heat peak narrows and for $h = H/k_B T = 5.37$ large values of specific heat are obtained only very near $T_c$. The resultant values for the points along the critical-field curve are compared with the "interface solution" in Fig. 9. Our estimated error bars are smaller than the size of the symbols plotted. The agreement with the "interface solution" is striking! Since this solution contains no constants or prefactors which may be slightly "corrected", we believe that the agreement with the Monte Carlo data is strong evidence that the solution is exact. Series-expansion results[27,60] are also plotted in Fig. 9 for comparison. The critical-field curves obtained from the series are unreliable for $H/|J_{NN}| \gtrsim 1$. The results obtained

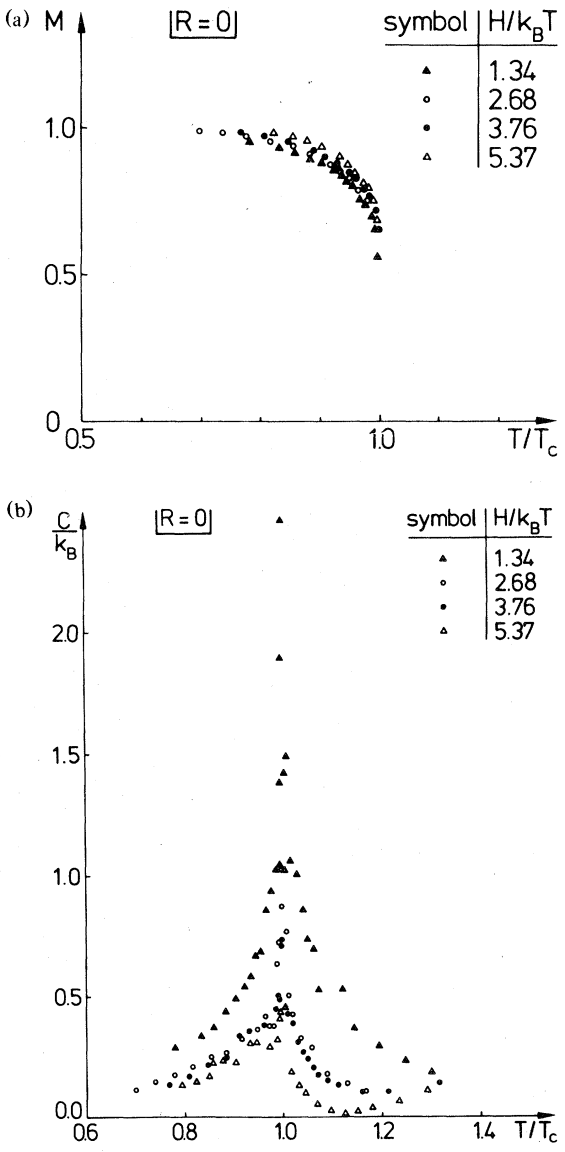


FIG. 8. (a) Magnetization plotted vs $T/T_c(H)$ for various values of $H/k_B T$ of the nearest-neighbor antiferromagnetic. (b) Specific heat plotted vs $T/T_c(H)$ for various values of $H/k_B T$.

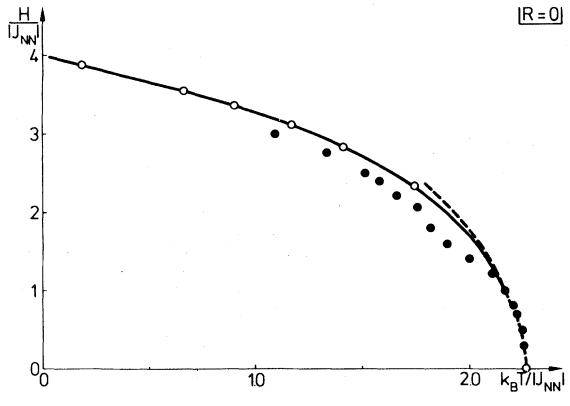


FIG. 9. Phase boundary of the nearest-neighbor Ising antiferromagnet in a magnetic field. The circles are the Monte Carlo results, the full curve denotes the "interface solution" (Ref. 25), the dashed curve gives series-expansion results (Refs. 27 and 60), while the dots denote the real-space renormalization results of Subbaswamy and Mahan (Ref. 23).

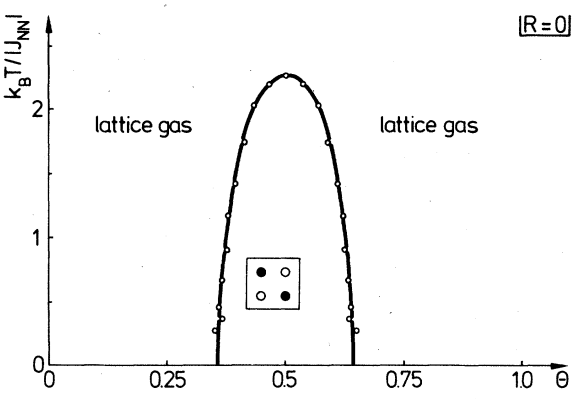


FIG. 10. Phase diagram of the lattice-gas model with nearest-neighbor repulsive interaction.

from a cell-cluster renormalization-group treatment[23] are also not in particularly good agreement with our data. The predicted $T_c(H=0)$, is too high, and the low-temperature portion of the critical-field curve is too low. Finally we note that Fisher's exact solution[62] for a "superexchange" Ising square lattice in a magnetic field yields a critical-field curve which falls off much faster from the $T=0$ value than does that for the ordinary square lattice.

The critical magnetization curve was also determined and is plotted as coverage versus temperature in Fig. 10. The critical magnetization at $T=0$ was estimated as $M_c=0.29\pm0.01$ and hence the ordered $c(2\times2)$ lattice-gas phase is stable at $T=0$ in the range 0.355–0.645. The lower value would correspond to the percolation limit and is in very good agreement with the value $\theta^*=0.371$ obtained assuming a noninteracting model with nearest-neighbor hard-core exculsion.

The adsorption isotherms for $R=0$ are shown in

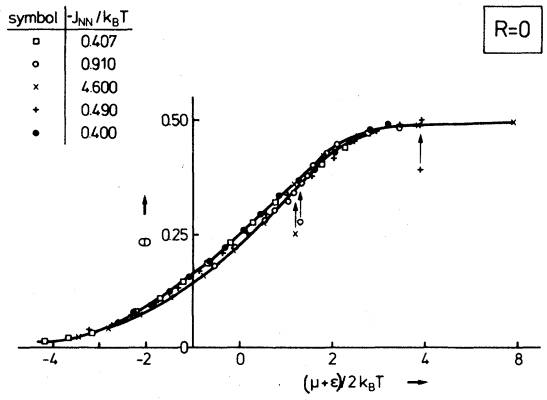


FIG. 11. Adsorption isotherms of the lattice-gas model with nearest-neighbor repulsive interaction at various temperatures. Arrows denote the points where the second-order phase transition from the ordered to the disordered phase occurs (cf. Fig. 10).

Fig. 11. The shapes of the isotherms are quite similar for all temperatures and, in fact, the curves are quantitatively quite similar as well.

## V. MONTE CARLO RESULTS ON PHASE DIAGRAMS AND THERMODYNAMIC PROPERTIES FOR $R>0$

It is already obvious from our discussion of ground-state properties (Sec. II) and the mean-field treatment (Sec. III) that for nonzero next-nearest-neighbor interaction, several orderings may compete and hence the analysis is much more complicated. It turns out that it is also much more complicated to obtain meaningful "data" from the computer experiment in this case. Particularly cumbersome is the proper distinction between phase transitions of first and second order in this case, a problem which strongly affects the phase diagram of the adsorbed-layer system[31] (in cases where first-order transitions occur, we have mixed-phase regions in a temperature-coverage diagram, cf. Fig. 6). Since this problem will be important for studies of other models as well, and errors have been made in our preliminary analysis,[7,31] we start by analyzing the difficulties occurring.

Figure 12 gives typical examples of our results taken on a $40\times40$ lattice with periodic boundary conditions and observation times $t$ in the range from 200 Monte Carlo steps MCS/spin to 3000 MCS/spin. First it must be noted that for low temperatures the results distinctly depend on the initial condition. E.g., in the case $R=\frac{1}{4}$ where for fields $H/|J_{NN}|<H_{c3}/|J_{NN}|$ ($=3$ in this case) the ground state is antiferromagnetic, we made runs starting at low fields with a perfect antiferromagnetic initial state, and then omit the first $\Delta t\approx\frac{1}{4}$ configurations and afterwards take an average over $t$ configurations. The last configuration of this run is used as an initial configuration for the next run with increased value of the field, etc. While some effects due to finite averaging times near phase transitions are familiar in Monte Carlo investigations,[63,65] in our case these observation time effects are unusually large. This observation can be understood by the fact that temperatures $T\ll|J_{NN}|$ have to be considered and hence for the reorientation of some small clusters of spins it may be necessary to overcome relatively high energy barriers. When one starts with fields appropriate for the disordered phase, using either a ferromagnetic or random starting configuration and then changes a field one often observes pronounced hysteresis of the order parameter. In addition, often the order parameter saturates at rather small values, which are not reproducible from one run to another where different random numbers are used, and which differ distinctly from the results obtained by starting in the ordered phase. Furthermore slight hysteresis in internal ener-

gy, magnetization is found which persists throughout the whole regime of the ordered phase. Inspection of the configurations reveals (Fig. 1) that these findings are explained by the fact, that during the observation time near the transition only incomplete ordering is achieved. Upon further changing the field (or temperature) the domain pattern is "frozen in". In the case of the $(2\times1)$ structure for $H > H_{c3}$ the antiphase domain boundaries between the domains of the $(2\times2)$ structure [Fig. 1(b)] do not cost any energy apart from "broken bonds" at the corners of the domains, as indicated in Fig. 1(b). The hysteresis in energy seen in Fig. 12 is due to these "broken bonds" and due to the difference in magnetization (via the Zeeman term in the Hamiltonian). The hysteresis in magnetization is due to the fact that formation of such a domain pattern often produces a slight "misfit" in the number of reversed spins which fit on our lattice. Thus the hysteresis seen in Fig. 12(b) (and similar hysteresis is seen in most of our data) is not taken as an evidence for a first-order phase transition but rather as an observation-time effect associated with a second-order phase transition.[64,65]

It turns out that in the regime $H_{c3} < H < H_{c4}$ $(R \leq \frac{1}{2})$ or $H_{c5} < H < H_{c4}$ $(R > \frac{1}{2})$ where in the ground state the degenerate structure described in Sec. II is stable, we never reached an order parameter corresponding to that structure which appreciably differed from zero. The reason is that for the "cooling velocities" (in the case of temperature changes) considered the frozen-in domain size still is distinctly smaller than the size of the sample. However, as long as domains of the arrangement of Fig. 1(a) and of that turned by 90° are present in the system, one has a cost in energy proportional to the domain interface—apart from the particular $(2\times2)$ arrangement, where one has an energy cost at the domain corners rather than edges, as noted above. Therefore only the latter arrangement is found as long as one obtains a multidomain sample. Although the lattice treated is quite small $(40\times40)$ it would be extremely time consuming to choose "cooling velocities" small enough that monodomain samples were obtained.[66] Thus we checked the ordering with respect to that structure by generating a structure as shown in Fig. 1(a) as an initial condition for runs at nonzero temperature. This is done by choosing a random number $\eta$ with $0 \leq \eta < 1$ for each antiferromagnetic row and starting it with an up spin if $\eta < \frac{1}{2}$ and with a down spin elsewhere. Even then it is found that the order parameter with respect to the one-dimensional antiferromagnetic rows is zero at nonzero temperatures. This is of course to be expected: if there were no disorder in the ferromagnetic rows (which is an excellent approximation for $T \to 0$), the antiferromagnetic rows can be treated as an ensemble of independent one-dimensional chains, which have a phase transition at $T = 0$ only. Hence at $T > 0$ there is no longer antiferromagnetic order in the "antiferromagnetic" rows but nevertheless there persists a $(2\times1)$

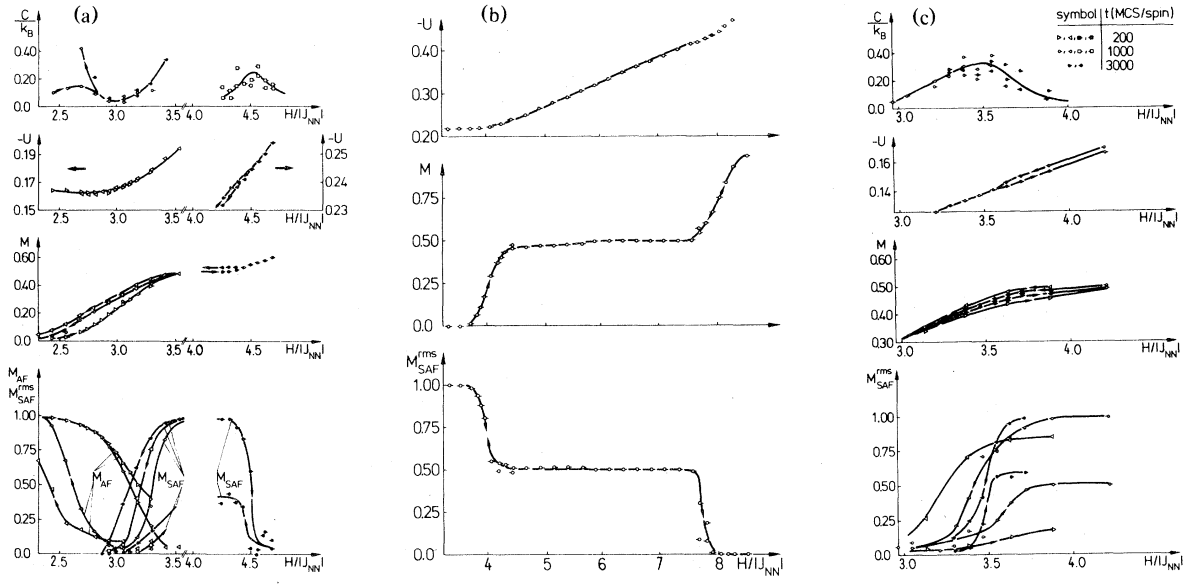


FIG. 12. "Raw data" for energy, specific heat, magnetization, and order parameters plotted vs field for $R = \frac{1}{4}$, $k_B T/|J_{NN}| = 0.273$ (a), $R = \frac{1}{2}$, $k_B T/J_{NN}| = 0.273$ (b), and $R = 1$, $k_B T/|J_{NN}| = 0.182$ (c), for various choices of the averaging time $t$. Curves are drawn to guide the eye (arrows at the curves indicates the direction of the field changes).

superstructure since the magnetization of the "antiferromagnetic" rows (which in the ideal case is zero) differs from the magnetization of the ferromagnetic rows (which in the ideal case is unity). The order parameter according to this "superantiferromagnetic" structure is included in Fig. 12. Our results suggest that the transition from this phase to the disordered phase is a second-order transition (taking into account the above interpretation of hysteresis in terms of domain effects and finite-observation-time effects).

An interesting question concerns the nature of the transition from this "superantiferromagnetic" structure to the ordinary superantiferromagnetic structure (where ferromagnetic rows alternate, which in the ideally ordered case have magnetization $\pm 1$, respectively), which is stable for $R > \frac{1}{2}$ and $H < H_{c5}$ in the ground state. Using the same arguments as above, at low temperatures this transition can be viewed as a change in mangetization (from $-1$ to 0) induced by the field in an ensemble of essentially independent one-dimensional rows (the rows with magnetization $+1$ act via the antiferromagnetic couplings like a negative field which produces a negative magnetization in the "antiferromagnetic" rows for $H < H_{c5}$). At nonzero temperatures the field-induced transitions in one-dimensional chains are continuous changes rather than phase transitions. This expectation is in fact borne out by the data [Fig. 12(c), Fig. 13]: even with rather short observation time ($t = 200$ MCS/spin) the "transition" at fields $H/|J_{NN}| \approx 4$ in Fig. 12(c) does not involve any hysteresis, in contrast to all other transitions [in particular, that at $H/|J_{NN}| \approx 7.5$ in Fig. 12(c)]. Thus although the two "transitions" seen in Fig. 12(c) look very similar at first sight, their interpretation is quite different. The snapshot pictures of spin configurations (Fig. 13) support our above description of this "transition" at $H/|J_{NN}| \approx 4$ as an essentially one-dimensional order-disorder phenomenon. Since both "phases" at low and high fields for $R > \frac{1}{2}$ have a structure with the same $(2 \times 1)$ periodicity, symmetry arguments[67] would predict a field-induced transition to be of first order, ending at a critical temperature $T_c$ where the transition is second order, while for $T > T_c$ the transition is a continuous change. This symmetry argument does not exclude our suggestion (which means $T_c = 0$ for this transition) but would exclude a line of critical points, of course. In the case of $T_c \neq 0$ one

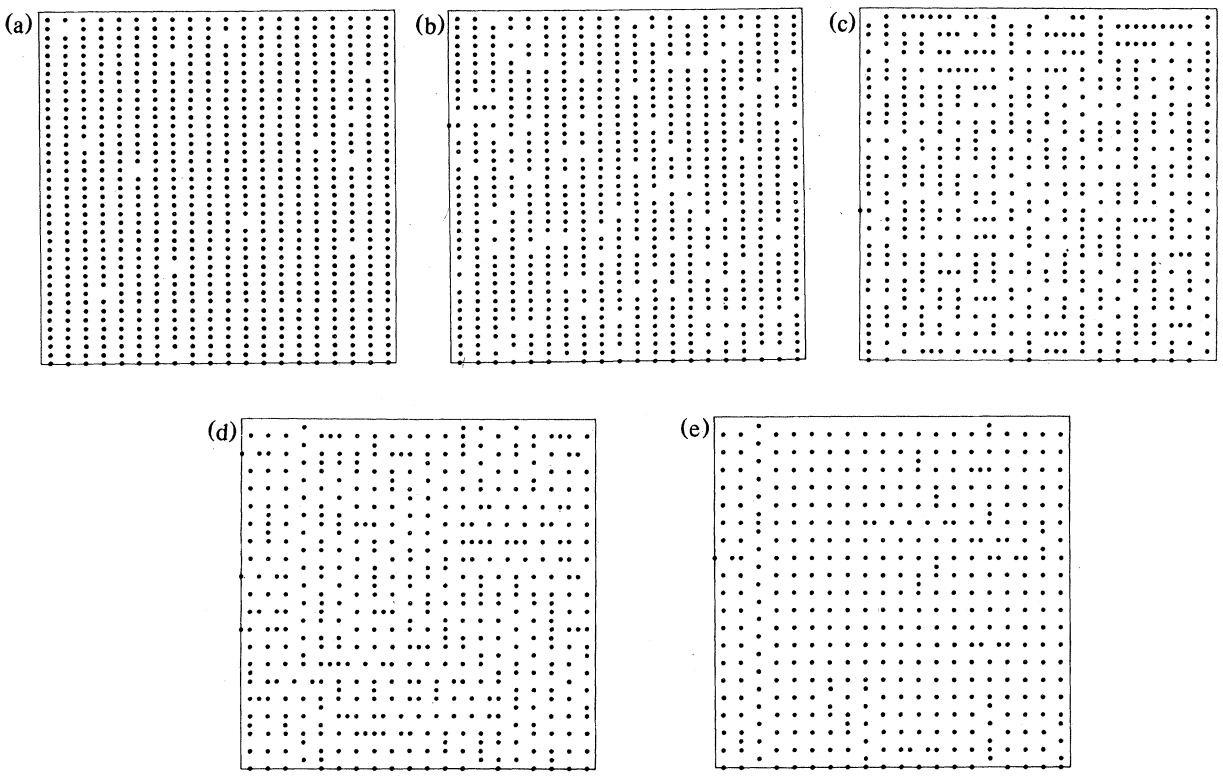


FIG. 13. "Snapshot pictures" of spin configurations of a $40 \times 40$ lattice with $R = 1$ at $k_B T/|J_{NN}| = 0.182$ for $2H/|J_{NN}| = 7.29$ (a), 7.66 (b), 8.02 (c), 8.39 (d), and 8.76 (e). Reversed spins are shown as black dots, up spins are not shown.

would expect for $T < T_c$ pronounced jumps of the magnetization of the "antiferromagnetic" rows and hence also pronounced hysteresis phenomena. We consider the absence of such phenomena as a strong evidence that only one superantiferromagnetic phase occurs for $T > 0$.

Even more tricky seems the question how the system transforms for $R < \frac{1}{2}$ from the simple antiferromagnetic phase at low fields to the "superantiferromagnetic" phase as the field is increased [Fig. 12(a)]. At first sight the very pronounced hysteresis seen there seems to imply phase transitions of first order. If there were a direct phase transformation from the one-ordered phase to the other as suggested on the basis of preliminary data,[7,31] the transition would necessarily be of first order by symmetry: there is no way to go from an antiferromagnetic order to a superantiferromagnetic order continuously. This is seen nicely, e.g., by describing the order in terms of a vector $\vec{M}$ with four components which are the magnetizations of the sublattices in that order.[68] Then it is obvious from Eqs. (4) and (5) that

$$\vec{M}_{AF} \cdot \vec{M}_{SAF}^{(1)} = M_1^2 + M_4^2 - M_2^2 - M_3^2 = 0 \ ,$$

since $M_1 = M_3$ and $M_2 = M_4$ in the antiferromagnetic structure, and since $M_1 = M_2$ and $M_3 = M_4$ in the superantiferromagnetic structure. Similarly also $\vec{M}_{AF} \cdot \vec{M}_{SAF}^{(2)} = 0$. Thus the ordering vectors of these two structures are orthogonal, and a continuous transition is only possible for $\vec{M}_{AF} = \vec{M}_{AF}^{(1,2)} = 0$, i.e., the paramagnetic phase.

Since in a four-component vector space there can be at most four mutually orthogonal vectors, and we also have

$$\vec{M}_{SAF}^{(1)} \cdot \vec{M}_{SAF}^{(2)} = \vec{M}_{SAF}^{(1)} \cdot \vec{M} = \vec{M}_{SAF}^{(2)} \cdot \vec{M} = \vec{M}_{AF} \cdot \vec{M} = 0 \ ,$$

it is clear that the four-sublattice structure of Eq. (7) is not orthogonal to any of the others in the above sense, but rather can be represented as a linear combination of all four other orthogonal orderings. Therefore one can have continuous transitions from any of the other structures to the four-sublattice structure without going through a point of paramagnetic phase. Such continuous transitions are in fact found in the mean-field treatment of Sec. III for the transition to the antiferromagnetic phase for small enough $R$.

From all these arguments it is not yet clear, however, that this first-order transition between antiferromagnetic and superantiferromagnetic phases actually occurs, because it may happen that one passes to an intermediate regime of disordered phase when the field is increased. We now interpret the fact that the "hysteresis loops" of the two order parameters overlap only weakly [Fig. 12(a)] as an evidence for this possibility. The same conclusion also results from our analysis of the transition as a function of magnetization at $T = 0$, Sec. II, where it was suggested that the antiferromagnetic order parameter increases at the critical magnetization from zero continuously: thus one would expect that there is a transition AF-P of second order for all $T \geq 0$. Another argument that the regime of the disordered phase extends down to $T \to 0$ at $H = H_{c3}$ stems from a consideration of interface energies at $T = 0$. For that purpose one considers a periodic $L \times L$ lattice with antiferromagnetic structure and calculates the excess of energy if the structure of $l$ adjacent rows is changed to be the $(2 \times 2)$ structures (both $L$ and $l$ have to be even numbers). One finds that the excess of energy is

$$\Delta U = Ll[-\tfrac{1}{2}H - 2(J_{NN} - J_{NNN})] + 2L[-\tfrac{1}{2}H - 2(J_{NN} - J_{NNN})] \ . \qquad (33)$$

The field $H$ where the coefficient of the volume term ($\propto Ll$) vanishes defines the critical field $H_{c3}$. It is seen that at $H_{c3}$ also the interface energy per spin (i.e., the coefficient of the term proportional to $2L$) vanishes. From these results one concludes that for $H = H_{c3} - \epsilon$ one can create "clusters" of the $(2 \times 2)$ structure of size $Ll$ which cost an energy of order unity only (due to the nonzero contribution of the corners only) if $\epsilon Ll \lesssim 1$. Therefore we expect that the order parameter of the antiferromagnetic phase goes to zero for any nonzero $T$ if $\epsilon$ is small enough. Since the same argument applies for clusters of the antiferromagnetic phase within the degenerate phase for $H = H_{c3} + \epsilon$, we conclude the regime of the disordered phase should extend to the point $(H_{c3}, T = 0)$.

The above considerations on the interpretation of our Monte Carlo data lead us to draw the phase diagrams as shown in Fig. 14. Comparing these results to the mean-field calculation (Fig. 4) we note a striking disagreement. While $H = 0$ and $R = \frac{1}{4}$, $R = 1$ the ordering temperature is overestimated by mean-field theory by about a factor of 2, the ordering temperature is overestimated by about a factor of 3 for fields $H > H_{c3}$ or $H > H_{c5}$, respectively. More important, mean-field theory fails to account for vanishing orderings due to degeneracy effects: it predicts ordered phases for $H < H_{c3}$ in the case $R = \frac{1}{2}$ and $H = H_{c3}$, $T > 0$ in the case $R < \frac{1}{2}$; it fails to describe correctly the SAF symmetry of the low-temperature phase for $H > H_{c3}$ ($R < \frac{1}{2}$) or $H > H_{c5}$ ($R > \frac{1}{2}$). Thus in all examples treated here even the wrong topology of the phase diagram results.

Considering now the phase diagrams of adsorbed layers (Fig. 15) the differences to the mean-field results (Fig. 6) are even more pronounced, since now the order of the various transitions crucially comes into play: the first-order transitions of mean-field theory lead to two-phase coexistence regions which are missing in Fig. 15 since we predict all transitions to be of second order. As expected, the stability of

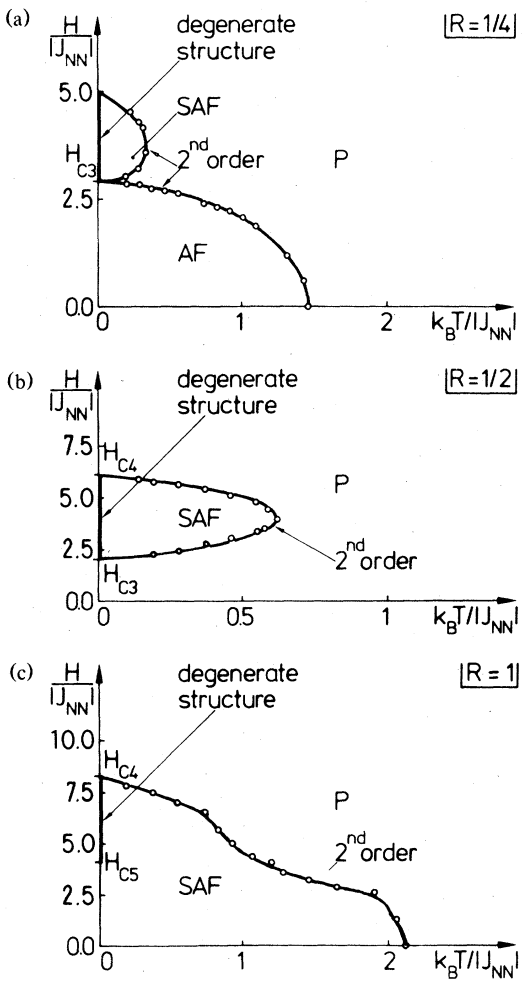


FIG. 14. Phase diagrams of the Ising square lattice with antiferromagnetic nearest- and next-nearest-neighbor interactions in a magnetic field for $R=\frac{1}{4}$ (a), $R=\frac{1}{2}$ (b), and $R=1$ (c). Phases occurring are paramagnetic (SAF), and the degenerate structure of Sec. II. Open circles denote Monte Carlo results for a $40\times 40$ system. All transitions are found to be of second order.

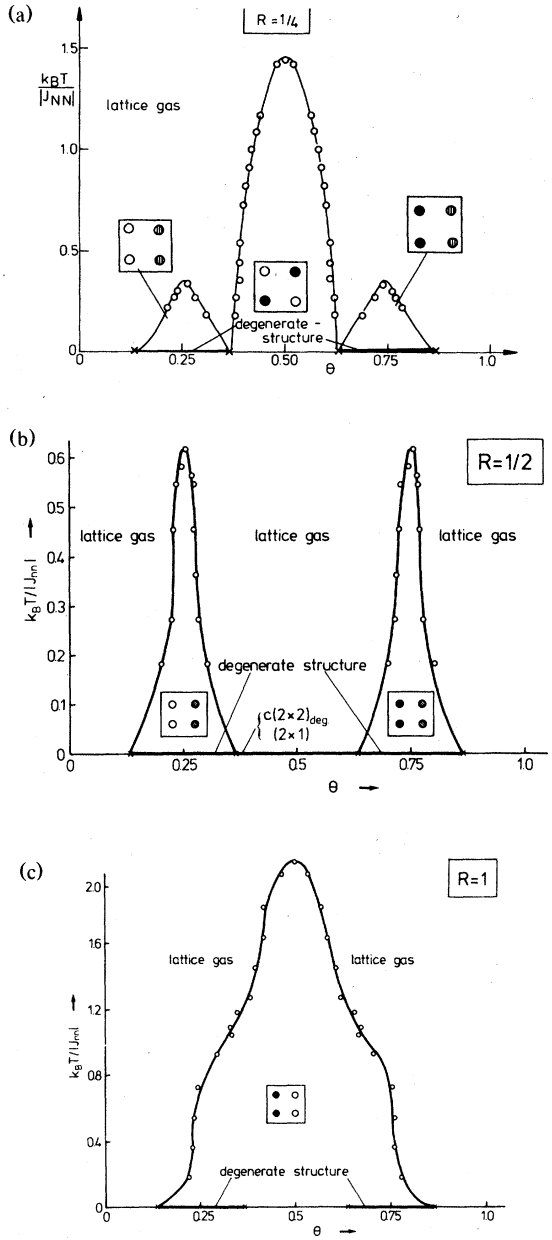


FIG. 15. Phase diagram of an adsorbed layer with repulsive nearest- and next-nearest-neighbor interactions for $R=\frac{1}{4}$ (a), $R=\frac{1}{2}$ (b), and $R=1$ (c). Elementary cells of the various occurring superstructures are indicated.

the ordered phases extends to the highest temperatures for those coverages where the ordering can be perfect ($\theta=\frac{1}{4}, \frac{1}{2}, \frac{3}{4}$).

Figure 16 finally gives our results for the adsorption isotherms obtains from the Monte Carlo calculation. It is seen that in the normalization chosen for low coverages the isotherm is independent of the interaction energy. Hence that regime is appropriately useful for a determination of the binding energy from experimental adsorption data, as expected. At higher coverages the adsorption isotherms depend on the interaction energies very sensitively, on the other hand. The *coverage* where deviations from temperature-independent behavior of the $\theta$ vs $(\mu+\epsilon)/k_BT$ relation set in is a measure for the *range* of the interaction, while the *temperature* where deviations set in is a measure for the *strength* of the interaction. While different ordering phenomena occurring give rise to different shapes of the isotherm, it is obviously hard to see any pronounced changes in the isotherm at the

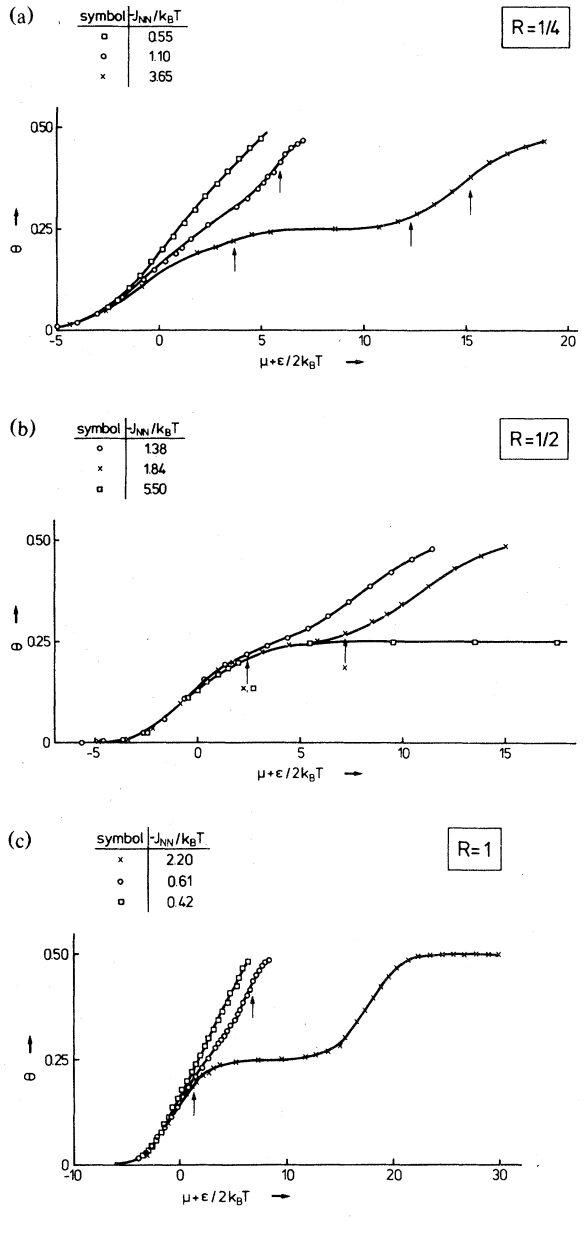


FIG. 16. Adsorption isotherms $\theta = \theta(\mu, T)$ calculated from Monte Carlo simulation for the adsorbed layers shown in Fig. 15. Arrows indicate the occurring second-order phase transitions.

coverages where a second-order transition occurs. Therefore mean-field theory yields some qualitative features of the adsorption isotherms correctly and fails dramatically only when first-order transitions and hence jumps in the isotherm are predicted (Fig. 7). Apart from the special case where the slope of the boundary $d\theta_c/dT$ diverges, one expects that the "susceptibility" $\chi = (\partial\theta/\partial\mu)_T$ diverges like the specific heat, and hence at the various transitions the slope of the adsorption isotherm should be infinite. Our results imply that this singularity either is visible in an extremely narrow regime around the transition, or the amplitude of the singular term is very small. Therefore in our finite lattice this singularity is then wiped out completely.

## VI. CRITICAL BEHAVIOR

In Secs. I–V we have concentrated on describing the general characteristics of the phase diagrams which result due to the application of a uniform magnetic field for a range of different $R$ values. Although we were primarily interested in determining the order and location of the phase transitions over the entire $H,T$ plane, we have also taken great care in studying the nature of the critical behavior near transitions which were clearly second order. From rather naive universality arguments we would be led to predict that the critical exponents assume the Ising square lattice values independent of $R$ or $H$. Recently, however, an analysis of possible ordered states using Landau-Lifshitz theory (but dropping the exclusion of third order invariants) has suggested[18,19] that the transition from the superantiferromagnetic to paramagnetic state belongs to the unversality class of the two-dimensional $xy$ model with cubic anisotropy. The critical exponents of this class are believed to be nonuniversal,[69] and we might thus expect to detect a dependence on $R$ and $H$. Previous studies[30] of the zero-field critical behavior for $R > \frac{1}{2}$ hinted at non-Ising behavior, but the data were simply not of sufficient accuracy to allow a meaningful, detailed analysis to be made.

In analyzing our results we shall make extensive use of the finite-size scaling theory developed by Fisher.[70] According to this approach, the thermodynamic behavior of a finite system near the infinite lattice $T_c$ can be described using a scaled variable $x = tL^{1/\nu}$ (where $t = |1 - T/T_c|$) and the infinite lattice critical exponents. For example, the order parameter and ordering susceptibility are given by

$$m = L^{-\beta/\nu} f(x) \quad , \tag{34a}$$

$$\chi^+ T = L^{\gamma/\nu} g(x) \quad , \tag{34b}$$

where, in the limit of $t \to 0$, $x \to \infty$, $f(x) \to Bx^{\beta}$, and $g(x) \to Cx^{-\gamma}$ so that the infinite-lattice critical behavior is recovered. The data may then be analyzed by assuming values for the exponents and testing the scaling behavior of the data using these exponent estimates. Finite-size scaling analyses[70–75] have been quite successful in analyzing critical behavior of several Ising models in two and three dimensions.

The data near the phase boundary for $R = 0$ have been tested for scaling behavior [using Eqs. (34a) and (34b)] for several values of $h = H/k_B T$, and in

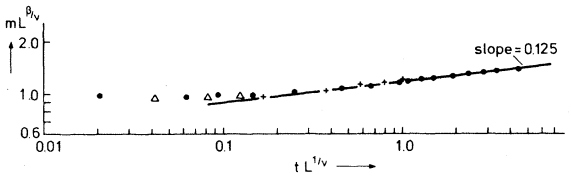


FIG. 17. Finite-size scaling plot of the order parameter for $R=0$ along a path of constant $h=H/k_BT=1.34$ ($k_BT_c/J_{NN}=1.743$). Data shown are: $L=20$, ●; $L=40$, Δ; $L=80$, +.

all cases the data were well described by scaling functions of the variable $x$ when the ordinary two-dimensional Ising exponents were used. As an example we show (Fig. 17) a finite-size scaling plot of the order-parameter data along a path of constant $H/k_BT=1.34$. Not only do the data fall upon a single, smooth curve, but for large $x$ the curve becomes linear with a slope equal to $\beta=0.125$. The critical amplitude obtained from the large $x$ behavior is $B=1.19\pm0.04$ and within experimental error is the same as the zero-field value[3] $B=1.22$. For paths of increasing $H/k_BT$ the critical amplitude slowly increases and for the steepest path studied in this way, $H/k_BT=5.37$ we find $B=1.29\pm0.04$.

Since earlier work[30] had indicated that the critical exponents for $R>>\frac{1}{2}$ were Ising-like, we chose to study the value $R=1$ in more detail. (We had also studied the phase diagram for this $R$ value). The specific-heat data for $R=1$ are shown for several values of $H$ in Fig. 18. For $H=0$ the specific-heat peak is very sharp. An examination of the finite-size behavior of the maximum values does not show the logarithmic size dependence which would indicate that the specific-heat exponent $\alpha$ is zero[70] (see Fig. 19). We analyzed the divergent portion of the specif-

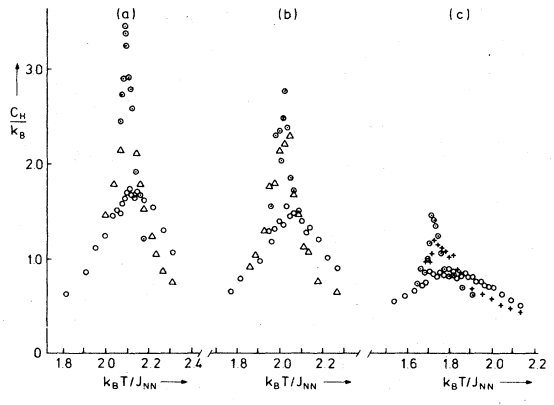


FIG. 18. Specific-heat data for $R=1$ along paths of constant $H$: (a) $H/J_{NN}=0$; (b) $H/J_{NN}=0.82$; (c) $H/J_{NN}=1.64$. Data are for: $L=14$, ○; $L=30$, +; $L=40$, Δ; $L=60$, ⊙.

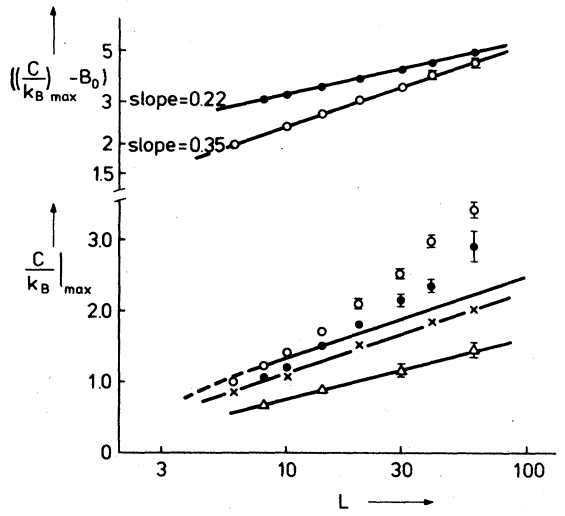


FIG. 19. Lattice-size dependence of the specific-heat maximum. (Below) semilog plots of $C_{max}$ vs $L$ for: $R=1$, $H=0$, (○); $R=1$, $H/J_{NN}=0.82$, (●); $R=1$, $H/J_{NN}=1.64$, (Δ); $R=5$, $H=0$, (×). The heavy line shows the $R=0$ result (Ref. 74). (Above) log-log plots of $C_{max}-B_0$ vs $L$ for: $R=1$, $H=0$, with $B_0=-1.0$ (○); $R=1$, $H/J_{NN}=0.82$, with $B_0=-2.0$, (●). The two lower lines in the lower part of this figure are fits to the data indicating logarithmic behavior.

ic heat by subtracting off a "background" $B_0$ which would provide linear behavior (with slope $=\alpha/\nu$) in a log-log plot such as that shown in the upper part of Fig. 19. Since rather large uncertainties exist in the choice of $B_0$, the errors in determining $\alpha/\nu$ are significant. The values of $B_0$ used in Fig. 19 were the smallest ones for which the variation over the entire size range appeared linear. For $H=0$ the slope $=\alpha/\nu=0.35$ with $B_0=-1$ and for $H/J_{NN}=0.82$ $\alpha/\nu=0.22$. Finite-size scaling analyses of the order parameter and ordering susceptibility for $H=0$ also show clear departure from Ising behavior. From the finite-size scaling plots shown in Figs. 20 and 21 we

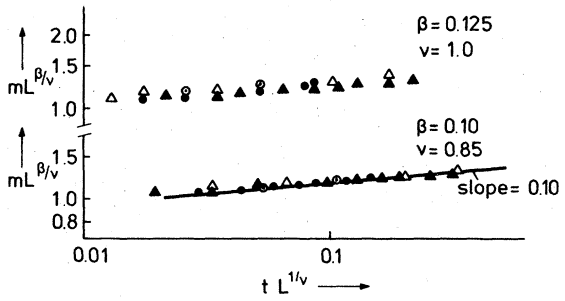


FIG. 20. Finite-size scaling plots of the order parameter for $R=1$, $H=0$ with two different choices of exponents. Data are for $L=10$, ▲; $L=20$, ●; $L=40$, Δ; $L=60$, ⊙.

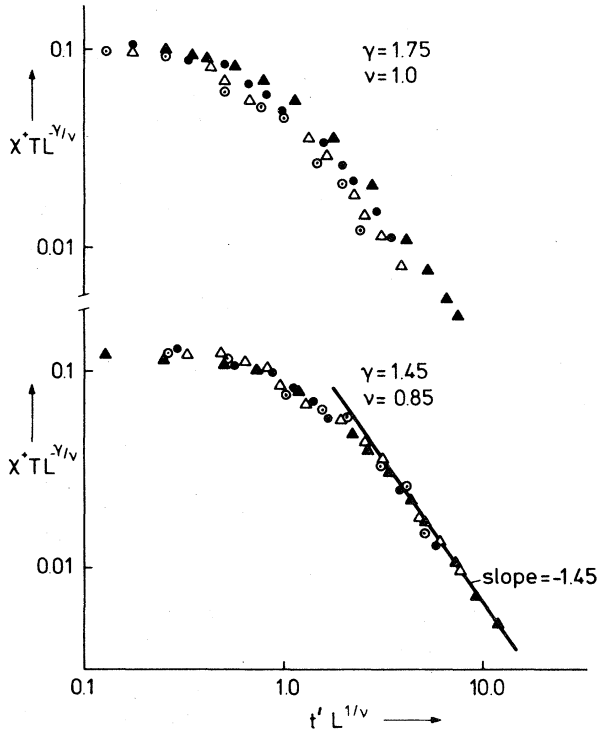


FIG. 21. Finite-size scaling plots of the high-temperature ordering susceptibility for $R=1$, $H=0$ ($k_B T_c/J_{NN}=2.08$). Data are for $L=10$, ▲; $L=20$, ●; $L=40$, Δ; $L=60$, ⊙.

see that the data can be made to scale quite well using the non-Ising exponents: $\gamma=1.45\pm0.10$, $\beta=0.10\pm0.02$, $\nu=0.85\pm0.05$. Note that the data clearly do not scale if Ising exponents are used instead. Combining this estimate for $\nu$ with our earlier result of $\alpha/\nu=0.35$ we now obtain $\alpha=0.30$. With the application of a magnetic field the critical behavior changes. The specific-heat peak is reduced, as shown in Fig. 18 and by the time $H/J_{NN}=1.64$ the size dependence of the maximum value is logarithmic (see Fig. 19) with an even smaller amplitude than that for $R=0$. For $h=0.82$, our estimates are $\nu=0.90\pm0.05$, $\gamma=1.55\pm0.10$, $\beta=0.11\pm0.02$, and $\alpha=0.20$. The finite size scaling plot for $H/J_{NN}=1.64$ shown in Fig. 22 shows that the data are well described by the Ising exponents $\gamma=1.75$, and $\nu=1.0$.

The data obtained for $R=5$ are also well described by Ising exponents. The size dependence of the specific-heat maximum is logarithmic (see Fig. 19), and a finite-size scaling plot of the high-temperature ordering susceptibility (Fig. 23) shows excellent scaling behavior with $\gamma=1.75$ and $\nu=1.0$. It is, of course, quite probable that the true exponents for both $R=5$, $H=0$ and $R=1$, $H/J_{NN}=1.64$ differ from the Ising values but by an amount which is

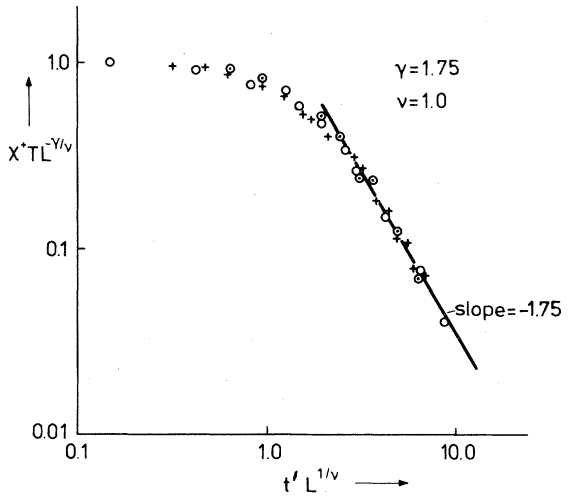


FIG. 22. Finite-size scaling plot of the high-temperature ordering susceptibility for $R=1$, $H/J_{NN}=1.64$ ($k_B T_c/J_{NN}=1.70$). Data are for $L=14$, ○; $L=30$, +; $L=60$, ⊙.

below our limits of resolution. We do wish to point out that for $R=5$, the normalized critical temperature $k_B T_c/J_{NNN}=2.255$ is very close to the value of $k_B T_c/J_{NNN}=2.269$ which must appear for $R=\infty$ when the interpenetrating NNN lattices are completely decoupled. Thus, our findings are consistent with a real-space renormalization-group treatment[76] as well as perturbation methods[77] which predict $R$-dependent exponents in this regime.

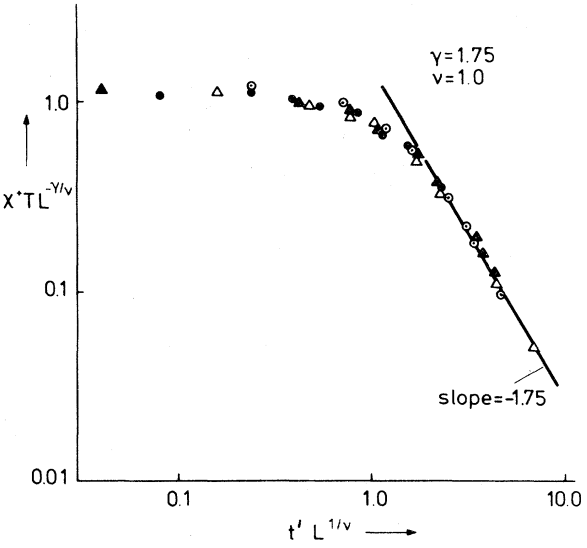


FIG. 23. Finite-size scaling plot of the high-temperature ordering susceptibility for $R=5$, $H=0$ ($k_B T_c=11.28$). Data are for $L=10$, ▲; $L=20$, ●; $L=40$, Δ; $L=60$, ⊙.

Since the critical exponents which we have obtained here are not constant, they obviously do not obey simple universality. As an alternative we have considered the possibility that "reduced" critical exponents, e.g., $\hat{\gamma}=\gamma/\nu$, $\hat{\beta}=\beta/\nu'$, $\hat{\phi}=(2-\alpha)/\nu$, etc., are constant according to Suzuki's idea of weak universality.[78] We find for $R=1$, $H=0$,

$$\hat{\gamma}=1.71\pm0.15\ ,\quad \hat{\beta}=0.118\pm0.020\ ,$$

$$\hat{\phi}=2.00\pm0.25\ .$$

For $R=1$, $H/J_{NN}=0.82$,

$$\hat{\gamma}=1.72\pm0.15\ ,\quad \hat{\beta}=0.12\pm0.02\ ,$$

$$\hat{\phi}=2.0\pm0.2\ .$$

For $R=1$, $H/J_{NN}=1.64$ and $R=5$, $H=0$, the reduced exponents are indistinguishable fom the $R=0$ values $\hat{\gamma}=1.75$, $\hat{\beta}=0.125$, $\hat{\phi}=2.0$. These results suggest that Suzuki's "weak" universality holds for this model.

We feel that this variation of critical exponents with $R$ and $H$ is a real effect and not just due to a crossover of Ising critical behavior to the multicritical behavior at the point $R=\frac{1}{2}$, $H=0$, where $T_c=0$ and the correlation length seems to increase exponentially fast as $T\to T_c=0$ (Ref. 30 ): The latter behavior would correspond formally to $\nu=\infty$, and hence the effective exponent $\nu_{\text{eff}}$ due to such a crossover should exceed $\nu=1$ distinctly, in contrast to what is found here.

## VII. CONCLUSIONS

In this paper we have considered Ising systems with antiferromagnetic nearest-neighbor interactions $J_{NN}$ and a wide range of competing next-nearest-neighbor interactions $J_{NNN}$ and have studied the magnetic field induced phase transitions. Our results show that simple tricritical behavior is limited to the regime $R=J_{NNN}/J_{NN}<0$. For $R=0$ our results for the second-order phase boundaries are (within experimental accuracy) identical to the prediction of Müller-Hartmann and Zittartz thus supporting the conjecture that the result is exact. For $0<R<\frac{1}{2}$ a degenerate phase is also found where ferromagnetic and antiferromagnetic rows alternate. We interpret the $T=0$ transitions as percolation transitions; hence the points $(H_C, T=0)$ are multicritical points. The $T=0$ transition from the degenerate to disordered phase is a generalized percolation transition but the resulting "percolation clusters" have nonunique structures. Remarkably, dynamic cooling of the system from the disordered phase to $T=0$ produces a metastable domain configuration of the simpler $(2\times2)$ structure but with an energy cost only at the *corners* of the domain. For $R>\frac{1}{2}$ only the degenerate phase exists. The critical exponents describing the transition to the disordered state are nonuniversal and appear to approach the two-dimensional Ising values only for large $R$ or $H$. We find that mean-field theory dramatically fails for several reasons to yield even all the qualitative aspects of some of the diagrams: (i) The free-energy differences between various ordered and disordered phases are extremely small over a wide range of temperature and field thus complicating analysis of the phase transitions; and (ii) mean-field theory cannot handle all of the degeneracy effects which make some of the transition temperatures go to zero.

It is tempting to speculate about what will happen when interactions of still longer range are added. If all interactions are repulsive, ordered phases with larger superlattice cells may be possible. If the third-nearest-neighbor interactions are attractive the "percolation point" $\theta^*$, will become a tricritical point on a phase boundary to the $(2\times2)$ structure which is then stable. $\theta_2^*$ should then be a triple point where the $(2\times2)$, $c(2\times2)$, and disordered phases coexist. Clearly then, in the case of competing interactions the phase diagrams are sensitive to both the strength and the range of the interactions.

## ACKNOWLEDGMENTS

This research was supported in part by the NSF and by NATO Research Grant No. 1185. We wish to thank Professor J. W. Cahn and Professor M. Schick for helpful comments and discussion.

[1]L. Onsager, Phys. Rev. 65, 117 (1944).
[2]C. N. Yang, Phys. Rev. 85, 808 (1952).
[3]B. M. McCoy and T. T. Wu, *The two-dimensional Ising model* (Harvard University, Cambridge, Mass., 1973).
[4]L. J. de Jongh and A. R. Miedema, *Experiments on Simple Magnetic Model Systems* (Taylor and Francis, London, 1974).
[5]H. Ikeda and K. Hirakawa, Solid State Commun. 14, 529 (1974).
[6]E. J. Samuelsen, J. Phys. Chem. Solids 35, 785 (1974).
[7]K. Binder and D. P. Landau, Surf. Sci. 61, 577 (1976).
[8]G. Doyen, G. Ertl and M. Plancher, J. Chem. Phys. 62, 2975 (1975); G. Ertl and M. Plancher, Surf. Sci. 48, 364 (1974); G. Ertl and J. Küppers, Surf. Sci. 21, 61 (1970).
[9]D. E. Andersson and S. Andersson, Surf. Sci. 23, 311 (1970).
[10]G.-C. Wang, T.-M. Lu, and M. G. Lagally, J. Chem. Phys. (to be published).
[11]W. Y. Ching, D. L. Huber, M. Fishkis, and M. G. Lagally (unpublished).
[12]J. C. Buchholtz and M. G. Lagally, Phys. Rev. Lett. 35, 442 (1975).
[13]G. Ertl and D. Schillinger, J. Chem. Phys. 66, 2569 (1977).

[14]J. G. Dash, Phys. Rep. 38C, 177 (1978), and references therein.
[15]B. Mihura and D. P. Landau, Phys. Rev. Lett. 38, 977 (1976); D. P. Landau (unpublished).
[16]A. N. Berker, S. Ostlund, and F. A. Putnam, Phys. Rev. B 17, 3650 (1978).
[17]E. Domany and E. K. Riedel, Phys. Rev. Lett. 40, 561 (1978); J. Appl. Phys. 49, 1315 (1978), and references therein.
[18]S. Krinsky and D. Mukamel, Phys. Rev. B 16, 2313 (1977).
[19]E. Domany, M. Schick, J. S. Walker, and R. B. Griffiths, Phys. Rev. B 18, 2209 (1978).
[20]J. S. Smart, *Effective Field Theories in Magnetism* (Saunders, London, 1966).
[21]S. Katsura and S. Fujimori, J. Phys. C 7, 2506 (1974).
[22]B. Nienhuis and M. Nauenberg, Phys. Rev. B 13, 2021 (1976).
[23]B. Schuh, Z. Phys. 31, 55 (1978); K. R. Subbaswamy and G. D. Mahan, Phys. Rev. Lett. 37, 642 (1976).
[24]W. Kinzel, Phys. Rev. B 19, 4584 (1979).
[25]E. Müller-Hartmann and J. Zittartz, Z. Phys. B 27, 261 (1977).
[26]T. W. Burkhardt, Z. Phys. B 29, 129 (1978); B. W. Southern, Z. Phys. B 30, 61 (1978).
[27]D. C. Rapaport and C. Domb, J. Phys. C 4, 2684 (1971); N. W. Dalton and D. W. Wood, J. Math. Phys. 10, 1271 (1969).
[28]R. W. Gibberd, J. Math. Phys. 10, 1026 (1969); C. Fan and F. Y. Wu, Phys. Rev. 179, 560 (1969); A. Kawasaki and T. Osawa, J. Phys. Soc. Jpn. Suppl. 26, 105 (1969).
[29]For details on this method see *Monte Carlo Methods in Statistical Physics (Topics in Current Physics, Vol. 7 )*, edited by K. Binder (Springer, New York, 1978).
[30]D. P. Landau, J. Appl. Phys. 42, 1284 (1971) and unpublished.
[31]Very few and preliminary results of the present investigation were given in Ref. 7, and in K. Binder and D. P. Landau, in *Proceedings of the Seventh International Vacuum Congress and the Third International Conference on Solid Surfaces*, edited by R. Dobrozemsky, F. Rüdenauer, F. P. Vieböck and A. Breth (Berger, Vienna, 1977), p. 811. Note, however, that Figs. 3 and 4 of this reference as well as Figs. 8 and 9 of Ref. 7 are partially inaccurate, as is discussed in Sec. V.
[32]L. K. Runnels, in *Phase Transitions and Critical Phenomena Vol. 2*, edited by C. Domb and M. S. Green (Academic, New York, 1972), p. 305, and references therein.
[33]P. J. Estrup, Phys. Today 28, No. 4, 33 (1975), and unpublished.
[34]J. A. Venables and P. S. Schabes-Retchkiman, J. Phys. (Paris) 38, C4-105 (1977).
[35]R. Schrieffer, in *Nobel Symposium 24, Collective Properties of Physical Systems*, edited by B. Lundquist and S. Lundquist (Academic, New York, 1973).
[36]W. Kappus, Z. Phys. B 29, 239 (1978), and references therein.
[37]K. Huang, *Statistical Mechanics* (Wiley, New York, 1963).
[38]M. J. Oliveira and R. B. Griffiths, Surf. Sci. 71, 687 (1978).
[39]One of us (K.B.) is indebted to Professor J. W. Cahn for a very helpful discussion on this point, and for pointing out some of the errors mentioned in Ref. 31.
[40]M. J. Richards and J. W. Cahn, Acta Metall. 19, 1263 (1971).
[41]S. J. Allen and J. W. Cahn, Acta Metall. 20, 423 (1972).
[42]T. Horiguchi and T. Morita, Phys. Lett. A 41, 9 (1972).
[43]J. Kanamori, Prog. Theor. Phys. 35, 16 (1966).
[44]Implicit assumptions that the ground state is the structure of Eq. (7) are also made in Refs. 7, 21, and 31.
[45]B. P. Metcalf, Phys. Lett. A 46, 325 (1974).
[46]M. Kaburagi and J. Kanamori, J. Phys. Soc. Jpn. 40, 291 (1976), and references therein.
[47]J. W. Essam, in *Phase Transitions and Critical Phenomena Vol. II*, edited by C. Domb and M. S. Green (Academic, New York, 1972).
[48]For a review, see L. K. Runnels, in Ref. 32.
[49]F. H. Ree and D. A. Chesnut, Phys. Rev. Lett. 18, 5 (1967)
[50]A. Bellemans and R. K. Nigam, J. Chem. Phys. 46, 2922 (1967).
[51]G. S. Rushbrooke and H. I. Scoins, Proc. R. Soc. London Sect. A 230, 74 (1955).
[52]D. S. Grant and M. E. Fisher, J. Chem. Phys. 43, 2840 (1965).
[53]H. E. Stanley, J. Phys. A 10, L211 (1977), and references therein.
[54]L. K. Runnels, J. P. Salvant, and H. R. Streiffer, J. Chem. Phys. 52, 2352 (1970).
[55]M. Suzuki and R. Kubo, J. Phys. Soc. Jpn. 24, 58 (1968).
[56]K. Binder, Phys. Rev. B 8, 3423 (1973).
[57]C. G. B. Garrett, J. Chem. Phys. 19, 1154 (1951).
[58]P. W. Kasteleijn, Physica (Utrecht) 22, 387 (1956).
[59]D. M. Burley, Physica (Utrecht) 27, 768 (1961).
[60]A. Bienenstock, J. Appl. Phys. 37, 1459 (1966); A. Bienenstock and J. Lewis, Phys. Rev. 160, 393 (1967).
[61]D. C. Rapaport (unpublished).
[62]M. E. Fisher, Proc. R. Soc. London Sect. A 254, 66 (1960); A 256, 502 (1960).
[63]K. Binder, in *Phase Transitions and Critical Phenomena Vol. 5b*, edited by C. Domb and M. S. Green (Academic, New York, 1976), p. 1.
[64]K. Binder, Adv. Phys. 23, 917 (1974); D. P. Landau, AIP Conf. Proc. 18, 819 (1974) and Ref. 29.
[65]D. P. Landau and K. Binder, Phys. Rev. B 17, 2328 (1978).
[66]This problem ought to be very cumbersome in simulations of spin glasses, where a highly degenerate and unknown ground-state structure is expected, cf. D. Stauffer and K. Binder, Z. Phys. B 30, 313 (1978), and K. Binder, J. Phys. (Paris) 39, C6-1527 (1978).
[67]L. D Landau and E. M. Lifshitz, *Statistical Physics* (Pergamon, New York, 1960).
[68]For a similar but independent analysis in the case of tetracritical points in mixed systems see S. Fishman and A. Aharony (unpublished).
[69]J. V. José, L. P. Kadanoff, S. Kirkpatrick, and D. R. Nelson, Phys. Rev. B 16, 1217 (1977).
[70]M. E. Fisher, in *Proceedings of the International Summer School Enrico Fermi 1970, Course 51, Varenna, Italy* (Academic, New York, 1971).
[71]K. Binder, Thin Solid Films 20, 367 (1974).
[72]D. P. Landau, Phys. Rev. B 13, 2997 (1976).
[73]D. P. Landau, Phys. Rev. B 14, 255 (1976).
[74]D. P. Landau, Phys. Rev. B 16, 4164 (1977).
[75]A. E. Ferdinand and M. E. Fisher, Phys. Rev. 185, 832 (1969).
[76]M. P. Nightingale, Phys. Lett. A 59, 486 (1977).
[77]M. N. Barber, J. Phys. A 12, 679 (1979).
[78]M. Suzuki, Prog. Theor. Phys. 51, 1992 (1974).